Universidad del País Vasco
Euskal Herriko Unibertsitatea

Máster Universitario en

Ingeniería **C**omputacional y **S**istemas **I**nteligentes

Konputazio Zientziak eta Adimen Artifiziala Saila –
Departamento de Ciencias de la Computación e Inteligencia Artificial

K I S A

I C S I

Tesis de Máster

Application of Advanced Regression Methods for Wear Prediction of Superalloys

Maialen Murua Etxeberria

Tutores

Roberto Santana
Intelligent Systems Group, Department of Computer Science and Artificial Intelligence
University of the Basque Country (UPV/EHU)

Iñigo Martínez
Instrumentation & Smart Systems
Tecnalia Research & Innovation

informatika fakultatea
facultad de informática

KZAA /CCIA

Septiembre 2016

Master Degree Thesis:

Application of Advanced Regression Methods for Wear Prediction of Superalloys

Maialen Murua Etxeberria

Advisors: Roberto Santana[(a)], Iñigo Martinez[(b)]

(a) Intelligent Systems Group, Department of Computer Science and Artificial Intelligence, University of the Basque Country UPV/EHU, Paseo Manuel de Lardizabal, 1 Donostia, 20018 Gipuzkoa, Spain.

(b) Tecnalia Research & Innovation, Instrumentation & Smart Systems Department, 20009 Donostia, Gipuzkoa, Spain.

m.muruaetxeberria@gmail.com

Abstract. Analytical models able to predict the tool wear can provide companies instruments to optimize the cutting processes. The focus of this thesis is to accomplish a study of the tool wear process in the turning process of superalloys, including its dependence on multiple factors related to the characteristics of the workpiece and machinery used for turning. As a natural extension of this study we propose the application of some statistical and machine learning techniques to address the prediction of the tool wear. Data corresponding to different tests carried out as part of the European project called Himmoval is used. The process of prediction involves selecting features from the variables acquired by different sensors that characterize the machining process. Additionally, several machine learning algorithms are implemented and applied to analyze the data from the wear experiments. Among these algorithms, Gradient Boosting Regressor predominates over the rest of regression methods evaluated.

Keywords: Tool wear prediction, advanced regression methods, turning of superalloys, PCA, hypothesis testing.

Acknowledgments

Firstly, I would like to express my sincere gratitude to my advisors Iñigo and Roberto for the continuous support of my master thesis, for their patience, motivation and knowledge. Specially to Roberto, his guidance helped me in all time of writing of this thesis. I would also like to thank Alfredo Suarez for his explanations and knowledge in the fabrication processes. But above everything for his motivation, without his help this thesis could not have been successfully conducted. My sincere thanks also goes to my workmates of Tecnalia who provided me an opportunity to feel as a part of their team.

Table of Contents

List of Figures

List of Tables

Abbreviations

HPC High Pressure Cooling. 11
HRSA High Resistant Superalloy. 10

LGA Large Grain Aged. 10
LGS Large Grain Solutioned. 10

PAA Piecewise Aggregate Approximation. 22

SGA Small Grain Aged. 10
SGS Small Grain Solutioned. 10

1 Introduction

1.1 Motivation

The use of superalloys in the hot sections of turbine machinery is nowadays very expanded. These alloys exhibit specific characteristics such as excellent mechanical strength, resistance to thermal creep deformation, good surface stability and resistance to corrosion or oxidation. Examples of such alloys are Inconel 718, Waspaloy and Haynes 282, that are composed by different chemical elements based on nickel [37]. As mentioned, the primary application of such superalloys is in gas turbines that are used to power aircraft, trains, ships, electrical generators or even tanks [44]. Other applications of superalloys are aerospace gas turbine engines, space vehicles, nuclear reactors, power generation turbines, submarines, petrochemical equipment, high-temperature fasteners, combustion engine exhaust valves and hot working tooling and dies. Three classes of alloys have appeared -cobalt-based, nickel-based, iron-based- to meet this superalloy definition [6].

Tool wear is an important factor which affects the machined surface characteristics, because during the machining processes those surfaces get more or less destroyed. Surface integrity is one of the most relevant parameters used for evaluating the quality of finish machined surfaces [2]. This destruction is decisive for the later characteristics of manufactured parts, therefore, tool wear estimation plays an important role. Tool wear estimation is not only a diagnosis to prevent tool failure or material waste but also to have better performance and service life of machined components [26]. In machining of nickel based superalloys, tool wear is a major problem due to the high stresses and the high temperatures at the tool chip interface [13]. Consequently, knowledge of the tool wear mechanism and the capability to predict tool wear are of great importance.

A noteworthy feature of nickel-based alloys is their use at temperatures in excess of 80% of their incipient melting temperatures, a fraction that it is higher than for any other class of engineering alloys. However, nickel-based superalloys are one of the extremely difficult-to-cut materials. During the machining process, the interaction between the machining tool and workpiece causes a severe deformation in the local area of the workpiece [66].

Alloy 718 (commonly called Inconel 718), and Waspaloy are both used for high temperature applications. Alloy 718 is a nickel-iron based superalloy and it is the most used superalloy that it is mainly applied in the hot section of turbine machinery and nuclear reactors. Waspaloy, a nickel-based superalloy is mainly used for parts in turbines such as compressor discs, shaft and turbine cases. Both materials are classified as difficult to cut materials and tool wear and tool life are major key factors when machining these alloys [35].

Haynes 282 alloy is a new (introduced in 2005) nickel-based superalloy developed for high temperature structural applications, particularly for aero and land-based gas turbine engines. A distinguishing characteristic of Haynes 282 is

its unique combination of remarkable creep strength, thermal stability and fabricability compared to the existing superalloys like Inconel 718 and Waspaloy [9].

In this thesis we apply machine learning techniques to study the tool wear effect in controlled experiments with different types of superalloys. We use real data collected as part of a European project devoted to the investigation of superalloys for machining processes.

1.2 Experimental framework

The project called Himmoval [1](high speed metallic material removal under acceptable surface integrity for rotating frame) is a European project whose aim is to develop a new rapid metal removal process under acceptable surface integrity for fabricating typical jet engine components made of high resistant superalloys. The Himmoval consortium is integrated by Tecnalia Research & Innovation, the University of the Basque Country and Geonx S.A.

The project has been developed in the applied research center, Tecnalia Research & Innovation [2] with the collaboration of the University of the Basque Country (UPV/EHU).

The Himmoval project consisted of a number of experiments in which different alloys were used for machining experiments and data about the different phases of the machining process were collected by sensors and stored in a number of databases for further analysis. Using this data some investigations [54] [56] [55] about cutting forces and tool wear in the three superalloys Inconel 718, Waspaloy and Haynes 282 were carried out. Some other studies were made about the improvement of cutting conditions and the variation of the wear pattern in high-pressure cooling of alloy 718.

1.3 Background

Machining is any of various processes in which a piece of raw material is cut into a desired final shape and size by a controlled material-removal process. The three principal machining processes are classified as turning, drilling and milling. When turning a piece of relatively rigid material, such as metal, it is rotated and a cutting tool is traversed to produce precise diameters and depths [5].

The wearing of the machining tool in the process of turning has been the subject of numerous studies and investigations. There are two different types of wear, flank wear and notch wear. The flank face is the surface over which the surface, produced on the workpiece, passes and that surface is where the flank

[1] `http://cordis.europa.eu/project/rcn/110875_es.html`

[2] Tecnalia Research & Innovation is a business company whose headquarters is in the Science and Technology Park of Bizkaia. Its activity is focused on the applied research with the objective of contributing to the society and other business companies with its research and awareness. It was created in 2010 as a result of the union of these companies: Cidemco, ESI, Euve, Fatronik, Inasmet, Labein, Leia and Robotiker.

wear occurs [11]. Flank wear is the most common type of wear and occurs due to abrasion, caused by hard constituents in the workpiece material. It starts at the cutting tip and then widens as the contact area increases, thus forming the wear land. The width, shape and growth rate of the wear land depend on the tool material, workpiece material and cutting parameters [51]. Notch wear is a common wear in machining of High Resistant Superalloy (HRSA). It is caused by adhesion (pressure welding of chips) and a deformation hardened surface. The notch wear appears outside the cutting depth [36].

One of the most promising techniques for tool wear detection and breakage involves the measurement of cutting forces [51]. The total force induced by the action of the cutting tool to the workpiece is called F. The resulting cutting force F breaks down into three components. The cutting force (F_y), is a component of the total force F in the direction of the cutting speed which is tangential. The other force F_z, is in the orthogonal direction of the cutting speed and it does not consume power (passive force). Finally, the component F_x is in the radial direction [59]. Changes in these forces indicate changes in machining parameters, such as depth of cut, feed rate, cutting speed and condition of tool [51].

In the particular experimental framework used in this thesis, the three superalloys will serve to investigate the effect of machining.

A heat treatment, heating and cooling are applied for the specific purpose of intentionally altering grain size and hardness. This process includes techniques such as annealing and precipitation hardening. This treatment is applied to the materials, Inconel 718, Waspaloy and Haynes 282 to obtain four different microstructures that differ on the grain size and hardness: Large Grain Solutioned (LGS), Large Grain Aged (LGA), Small Grain Solutioned (SGS) and Small Grain Aged (SGA). In the case of Haynes 282, it only reaches the states of LGS and LGA.

In Table 1, grain size and microhardness values for all considered superalloys are shown.

Alloys	Properties	LGS	LGA	SGS	SGA
Haynes 282	Grain size	150-330	93-280		
	Microhardness	190	362		
Waspaloy	Grain size	140	180-320	50-60	20-30
	Microhardness	278	455	287	441
Inconel 718	Grain size	160	130	16-30	15-32
	Microhardness	240	493	296	497

Table 1: Grain size and microhardness for the three alloys investigated in all states considered.

In metal cutting there are many factors related to process planning for machining operations. These factors can be classified as: Type of machining operations (turning, milling etc.), parameters of machine tools (rigidity, hardness etc.), parameters of cutting tools (material, geometry etc.), parameters of cutting conditions (cutting speed, feed rate etc.) [41]. The cutting parameters of the transverse turning operation used in all the experiments considered in thesis are the same: entering angle (91°), rake angle (0°), inclination angle (0°), nose radius (0.4 mm), cutting speed (30 m/min), feed rate (0.1 mm/rev) and cutting depth (2 mm).

The turning process involves generation of high cutting forces and temperatures, and lubrication becomes critical to minimize the effects of these forces and temperature on the cutting tool and workpiece. In this case, the conventional and High Pressure Cooling (HPC) were used. The primary objective of delivering coolant under high pressure is to reduce the temperature generated in the cutting region to extend the tool life [66]. The temperature is measured with two sensors called Thermocouple 1 and Thermocouple 2.

1.4 Description of the databases

The databases store data from the experiment described in the previous section. Some of the variables of the databases such as the forces and temperature are measured as a time series, that is to say that we have a sequence of data points over a time interval. A time series is a sequence of observations, usually ordered in time and the feature that distinguishes from other statistical analysis is that successive observations may be dependent [1].

The variables of the database are the following ones:

- Flank wear maximum (quantitative)
- Flank wear mean (quantitative)
- Notch wear (quantitative)
- Chips meter (quantitative)
- States (qualitative): LGS, LGA, SGS, SGA.
- Material (qualitative): Inconel 718, Waspaloy, Haynes 282.
- Temperature (quantitative): It is measured with two sensors. Thermocouple1 and Thermocouple 2.
- Lubrication (qualitative): Without lubrication, conventional, HPC.
- Forces (quantitative): F_x, F_y, F_z.

Flank wear maximum: It is measured after each of the passes, in nine points of the tool, and the maximum value of the wear among the nine points of the tool is assigned to this variable. A variable transformation is made from the original discrete variable to a continuous one.

Flank wear mean: As occurs in the case of flank wear maximum, the mean of the nine points is calculated and a variable transformation is made from the original discrete variable to a continuous one.

Notch wear: It is measured only at the maximum value of the wear and it is interpolated linearly.

Chips meter: Table 2 and Table 3 show the initial diameter and final diameter (mm) of each of the passes and superalloys. The variable chips meter measures the spiral cutting length (SCL), and it is the product of the machining time of each pass and cutting speed (30 m/min).

	Initial diameter (mm)	Final diameter (mm)	Spiral cutting length (m)
First pass	126	21	121,23
Second pass	126	21	121,23
Third pass	126	21	121,23
Four pass	126	21	121,23
Five pass	126	21	121,23
Six pass	126	21	121,23

Table 2: Chips meter in Inconel 718 and Waspalloy.

	Initial diameter (mm)	Final diameter (mm)	Spiral cutting length (m)
First pass	152	21,5	178.78
Second pass	152	22	178.61
Third pass	152	22,5	178.44
Four pass	152	23	178.26

Table 3: Chips meter in Haynes 282.

States: Four states are considered in the case of Inconel 718 and Waspaloy (LGS, SGS, LGA and SGA) and two states in the case of Haynes (LGS and LGA).

Material: The superalloys used in the experiments are: Inconel 718, Waspaloy and Haynes 284.

Temperature: It is measured as a time series in the variables Thermocouple 1 and Thermocouple 2. It is available only in Inconel SGA state.

Lubrication: Two types of lubrications are contemplated: normal and HPC.

Forces: The forces are measured as a time series in the variables F_x, F_y and F_z.

A test is a repetition of the process of turning involving 6 passes for a specific lubrication, state and material. There were carried out different tests changing the superalloy types and other parameters of the turning process to measure the variables. In some cases there is more than one test using exactly the same material and machining parameters and the values of temperature were measured

only in the Inconel 718 material and SGA state. Tables 4, 5 and 6 show the description of all available tests for each of the superalloys.

Material	State	Lubrication	Number of Tests
Inconel 718	LGA	Conventional	2
		HPC	2
	LGS	Conventional	3
	SGA	Conventional	3
		Dry	1
		HPC	3
	SGS	Conventional	2

Table 4: Description of available tests for Inconel 718.

Material	State	Lubrication	Number of Tests
Waspaloy	LGA	Conventional	2
		HPC	3
	LGS	Conventional	1
		HPC	1
	SGA	Conventional	2
		HPC	2
	SGS	Conventional	2
		HPC	1

Table 5: Description of available tests Waspaloy.

Material	State	Lubrication	Number of Tests
Haynes 282	LGA	Conventional	2
		HPC	1
	LGS	Conventional	2
		HPC	1

Table 6: Description of available tests Haynes 282.

2 State of the Art

2.1 Methods for modeling machining processes and parameters

The prediction of cutting behavior of processes and optimization of machining parameters have been the subject of diverse research [43] [20] [29] and the predictions of cutting force and tool life in machining have become a challenging task for proper optimization of the process, mainly because they play an important role in the economic aspects of metal cutting operations [10]. In a turning process the cutting parameters (cutting speed, feed force and depth of cut) should be optimized for achieving the minimum cost of machining and minimum production time. Nonetheless, for efficient optimization it would be useful to understand how the cutting parameters influence the process and this can be posed as a prediction problem.

One of the facets of quality of a turned piece is surface finish. Surface finish is defined as the degree of smoothness of a part's surface after it has been manufactured. Researchers studied the effect of different factors such as feed rate, cutting speed, depth of cut, work materials characteristics, etc. on surface finish. For modeling machining parameters, some scholars have proposed [32] [15] the use of soft computing techniques to carry out research. There are important contributions based on Artificial Neural Networks (ANN), Bayesian Network (BN), Multiple Regression (MR) and Response Surface Methodology (RSM) [66].

An artificial neural network is capable of learning from an experimental data set to describe nonlinear effects between input and output variables with great success. An ANN is defined by input and output layers, weight vectors and an activation function. A neural network is trained with a dataset and tested with a different dataset to arrive to an optimal topology and weights. Once trained it can be used for prediction. The advantage of ANN models is that they are capable of representing both linear and non-linear relationships and are able to learn these relationships directly from the data being modeled. Tool wear is a very complicated process associated with several parameters. Therefore, ANN is an appropriate technique for developing tool condition monitoring systems [26]. The major limitation to the use of neural networks is that it requires a large set of experimental data [10].

In addition to their application to tool condition monitoring [26], ANNs have been used to predict some other characteristics of the tool. In an experiment conducted to predict surface roughness [14] in high speed machining, Bayesian network and ANN were applied to classification. Seven variables measured in the milling process were taken to construct the Bayesian network and the average surface roughness was chosen as the class variable. The comparison of the two approaches was done using the indicators: False Positive, False Negative, True Positive, True Negative and Accuracy. An analysis of these measures indicated the superiority of the Bayesian network over the ANN for this problem.

An early work that addresses the prediction of machining performance using neural networks is by Rangwala and Dornfeld [43]. They used a feedforward network model to predict the cutting performance in the turning process. The network is trained using different input variables: cutting speed, feed rate and depth of cut; and output variables: cutting force, temperature, power and surface finish. Rangwala and Dornfeld [43], as many other researchers, utilized Multilayer Perceptron (MLP) neural networks for machining performance prediction. An MLP neural network consists on (apart from input and output layer) more than one hidden layers [10].

Regression is a conceptually simple technique to investigate relationships between input and output decision variables. Although statistical regression may work well for modeling, this technique may not describe precisely the non-linear complex relationship between the decision variables and responses. It is only an auxiliary way to confirm cause-effect relationship, and does not imply a cause and effect relationship. Moreover, error components of the regression equation need to be independent, normally distributed and having a constant variance.

Several researchers have compared the effectiveness of the neural network model with statistical regression models. Chryssolouris and Guillot [12] observed the superiority of the neural network model compared to the regression model. On the other hand, Feng and Wang [20] found multiple regression analysis and neural networks equally effective in predicting surface roughness for a finish turning process.

Analysis of variance (ANOVA), can be helpful for determining the effect of any given input parameter from a series of experimental results. ANOVA is a collection of statistical models, and their associated procedures, in which the observed variance in a particular variable is partitioned into components attributable to different sources of variation. In its simplest form, ANOVA provides a statistical test of whether or not the means of several groups are all equal, and therefore generalizes t-test to more than two groups [29].

In an investigation for estimating flank wear in turning Inconel 718, Yadav, Abhishek and Mahapatra [63] used ANOVA to identify most influencing variables on tool wear and material rate. This analysis suggested that most influencing factors were spindle speed, depth of cut and feed rate in case of material removal rate though, spindle speed and depth of cut were more important in case of flank wear.

PCA, has been widely utilized in system identification and dimensionality reduction in dynamic systems and it is an efficient approach to extract features from sensory signals acquired form multiple sensors [50]. In [49], principal component analysis was used as a feature extraction for investigating chip formation in the turning process. The chip formation was measured through cutting force components and radial displacement. Combining different cutting parameters, a total of 90 turning tests were performed. To implement PCA, data adjustment was carried out by centering the mean of the data set. The 4 and 3 principal

components, obtained through PCA application were used as an input features in model construction and the models constructed with 4-element feature vectors perform better than 3-element feature vector cases.

In a similar investigation [48] made about tool state in high performance cutting of nickel superalloy, PCA was applied to the sensor signals generated during cutting process. The aim was to reduce the high dimensionality of data, consisting of a large number of interrelated variables by extracting significant signals features. Principal component analysis was an efficient approach to extract features from sensory signals acquired from multiple sensors.

Dubey and Yadava [16] applied a multi-objective optimization of a laser cutting of superalloy using PCA. The primary objective of the study was to achieve an optimum parameter level that improves multiple quality characteristics at the same time. Firstly single-objective optimization was performed using Taguchi method (TM) and then TM combined with PCA was used for multi-objective optimization. The predicted optimum parameter levels were in good agreement with the results of the experiments.

Some other researches [51] [11] have investigated the relationship between tool wear and force ratio (ratio between the feed force and the cutting force components). Choudhury and Kishore [11] presented a mathematical model of tool wear as a function of force ratio, cutting speed, feed, depth of cut and diameter of the workpiece using experimental data. Tool wear was estimated with this model and verified by conducting a series of experiments. In the mentioned investigation the authors concluded that the mathematical model correlating force ratio and flank wear performed successfully.

Sikdar and Chen [51] described the relationship between flank wear area and cutting forces for turning operations. The experimental results showed that there was an increase in the three directional components of the cutting force with increase in flank wear area. Among the three cutting forces measured, the tangential force was the largest while the radial force was the smallest. However, when the tool began to fail, all cutting forces increased sharply, especially for the axial and radial forces. The radial force was found to be slightly larger than axial force when the tool began to fail [51].

In some investigations [30] [61], wear rate models have been used to estimate tool wear. In a research work carried out to estimate wear of ceramic and coated carbide tools in turning of Inconel 625 Usui's wear rate model was used [64]. This model was based on the equation of adhesive wear, which involves temperature, normal stress, and sliding velocity at the contact surface. As input parameters, feed rate, cutting speed and depth of cut were considered. The comparison of tool wear rate showed that predicted and experimental values were in good agreement.

There are a variety of studies [53] [50] [52] [42] that use support vector machine (SVM) technique to predict flank wear Shi and Gindy developed a new

tool wear predictive model by combination of least squares support vector machines (LS-SVM) and PCA technique [50]. PCA was firstly applied to extract features from multiple sensory signals acquired from machining processes. Then LS-SVM-based tool wear prediction model was constructed by learning the correlation between extracted features and the actual tool wear. A good agreement it was found between predicted tool wear constructed by the proposed method and the measured tool wear.

In machine learning, support vector machines are supervised learning models with associated learning algorithms that analyze data used for classification and regression analysis. In these methods, the data is mapped into higher dimensional input space and an optimal separating hyperplane is constructed in the mentioned space. Kernel functions and parameters are chosen such that a bound on the VC dimension is minimized [57]. SVM is a novel machine-learning tool especially useful for the classification and prediction with small-sample case [58].

Finite element method (FME) have been also used as a modeling strategy. FME is a numerical technique that it is used to find the solutions of partial differential equations [67]. FME splits a larger problem into a simpler problems called finite elements. This method approximates solutions by minimizing the associated error function. In [60], an FE-based approach was used for modeling a turning process of Inconel 718, specifically to predict the cutting force. In [64], FME was used to modify the parameters of Usui's model.

Kilundu, Dehombreux and Chiementin explored the use of data mining techniques for tool condition monitoring in metal cutting [27]. To recognize tool condition, five classes were defined to classify the 22 signals monitored in the experiment. Four classification methods were tested on the data set: Decision trees, Bayesian networks, k-nearest neighbour and neural network. The classification results were assessed by mean of a confusion matrix. The classification method that perform best was neural network followed by k-NN, decision tree and Bayesian network. Before the classifying process feature extraction and selection were carried out. Feature selection was done by using discriminant analysis to allow a better class separation.

The manufactures ultimate goals are to produce high quality product with less cost. Although we have mentioned before some prediction techniques, one of the considerations is the optimization of the machining parameters. Yusup, Zain and Hashim [65] reviewed several evolutionary techniques in machining parameters. They focused on meta-heuristic algorithms such as, genetic algorithm (GA), simulated annealing (SA), particle swarm optimization (PSO), artificial bee colony optimization (ABC) and ant colony optimization (ACO). The authors found that GA optimization was widely used followed by PSO, SA, ABC and ACO. They also reported that GA and PSO were mostly used for Multipass-turning whereas the most machining processes considered in SA was milling.

Approach	Application	Reference
Multiple Regression	Prediction of surface roughness in finish turning process	[20]
Polynomial Regression	Relationship between tool flank wear and component forces in turning	[51]
Neural Networks	Prediction in cutting performance in turning process	[43]
Neural Networks	Modelling the correlation between cutting and process parameters	[19]
ANN, genetic algorithm and fuzzy logic	Prediction of surface quality in machining process	[31]
Bayesian network (BN) and ANN	Prediction of surface roughness in milling process	[14]
ANN, BN, k-NN and decision tree	Prediction of tool conditioning monitoring in metal cutting	[27]
Analysis of means (AOM) and ANOVA	Effect of machining parameters and cutting edge geometry on surface integrity	[38]
ANOVA	Optimization of process parameters in turning operation	[29]
PCA	Feature extraction in sensor monitoring of chip form during turning	[49]
PCA	Multi-objective optimization of laser cutting	[16]
Finite element method (FEM)	Estimation of wear of ceramic and coated carbide tools	[30]
Support vector machine (SVM)	Tool wear prediction model for a machining process	[50]

Table 7: Soft computing approaches to machining.

In Table 7, we present a summary of some techniques applied to the analysis, modeling, and optimization of machining processes. In section 6 we propose the application of a variety of machine learning methods for predicting flank wear in the turning of Inconel 718. Our approach considers the application of advanced regression methods using as input variables features selected from the cutting forces.

2.2 Analysis of superalloys properties

Alloy 718, is today one of the most used superalloys, specially applied in the hot section of turbine machinery. This nickel-iron based superalloy has attracted considerable research in the improvement of tool materials, machining parameters and the cutting speed and feed rate [36]. Some studies indicate [35] that there is a correlation between grain size and notch wear. It is considered to be of interest to examine if such a grain size effect on notch wear could be independent of the hardness [35].

Olovsjö, Wretland and Sjöberg [36] determine the effect of grain size and hardness on the wear of the machining tool in an experiment carried out with Alloy 718. The authors reached the conclusion that for the materials with large grains (LGS and LGA) the notch wear was much more predominant than the two materials with small grains. The same authors also reported that hardness had a strong influence on flank wear and little if any influence could be attributed to the grain size. Nevertheless the general conclusion was that flank wear is not related to grain size and the conclusion may also be drawn that the hardness associated with a smaller grain size at least does not increase wear [35].

Some investigators [54] studied the influence of cutting forces and tool wear in turning of Haynes 282. The researchers concluded that mean flank wear propagates at a higher rate in machining LGA state than in machining of LGS state. Thus, an important influence of the hardness of the material on flank wear was observed. In the case of LGA state the mean flank wear was observed to be more randomly propagated. The most significant type of wear that occurs is notch wear. The propagation of the notch wear is then stable and predictable growing with increasing spiral cutting length (increasing number of passes). As it was observed in the case of the flank wear the LGS state shows to be more stable. For both states, the notch wear is much larger than the flank wear when turning Haynes 282 and notch wear is always higher in the case of LGA but it progresses as fast as in the case of LGS. The notch wear in the case of Haynes 282 is at least as aggressive as in the case of other nickel-based alloys [54].

The studies of the mentioned superalloys were based on the visualization of flank and notch wear and the conclusions of the relation of those wears with the size and microhardness were not supported with statistical analysis. We are going to investigate the relationship between superalloys characteristics (grain size and hardness) and flank wear. In doing so, we will use a different approach to those previously applied. Our approach is based on statistical hypothesis testing exactly Wilcoxon signed-rank non-parametric test. Other statistical approaches such as PCA are used to have a detailed vision of the problem that will be helpful for the prediction of the wear. Finally, we will also show that the influence of the different states of size and microhardness on wear can be analyzed by contrasting the results of regression for predicting wear for superalloys with different components.

3 Exploratory Data Analysis

A necessary step for the conception of a model of a process is an exploratory analysis of the data. This step can include dimensionality reduction, visualization, and preliminary regression and statistical tests to characterize the relationships between the variables of the modeled problem.

In this section the analysis will be focused on the forces involved in the turning process of Inconel 718, and for this purpose Inconel 718, LGA, HPC,

test 1 and test 2 will be used. We will start with an initial exploration of the data and continue with a deeper analysis.

3.1 Initial exploration of data

In this section we will carried out an initial exploration of the data analyzing the time series of the forces. In the analyzed databases there are approximately 514.000 points for each variable and each of the passes. In the experimental trials after each of the passes the process of turning has been stopped. As a result, in the beginning and at the end of each pass the force increases and decreases significantly as we can see in Fig. 1. In that figure, there are shown the three forces versus chips meter. F_x and F_y take bigger values, specially F_y, whereas F_z takes values lower than 200.

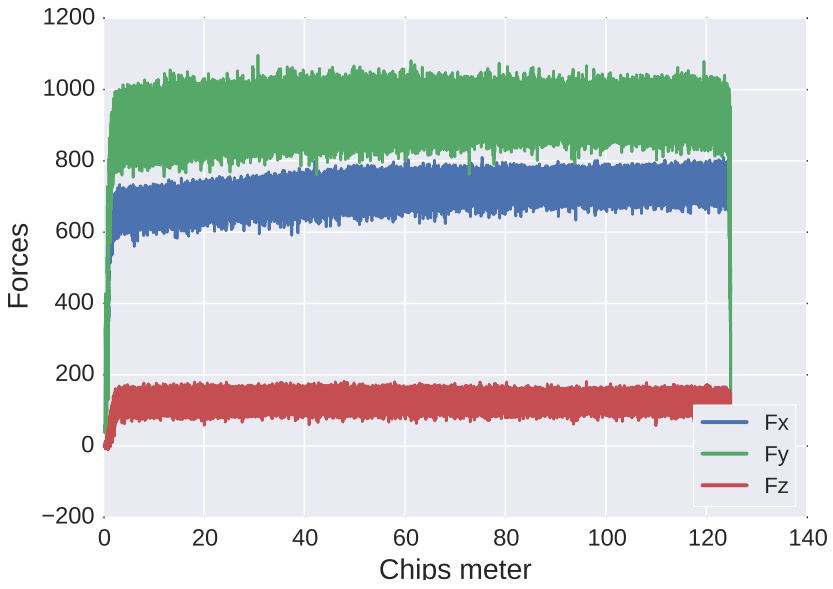

Fig. 1: Forces of the cutting tool in experiments with Inconel 718, LGA, HPC, Test 1, Pass 1.

This analysis has indicated us the necessity to filter the data in order to remove all those insignificant points (the peaks in the beggining and at the end of the pass). We define an interval of values that defines data that will be considered as relevant and those points out of the interval will be removed. In Equation 1, μ is the mean of the forces, σ is the standard deviation and k a

positive constant value. We will use $k = 3$. Points below the interval shown in Equation 1 will be removed.

$$thr = \mu - k\sigma \tag{1}$$

In Fig. 2. we can see the original data and the data after preprocessing for Inconel 718, LGA, HPC, T2. All the analysis considered from here on has been carried out using filtered data.

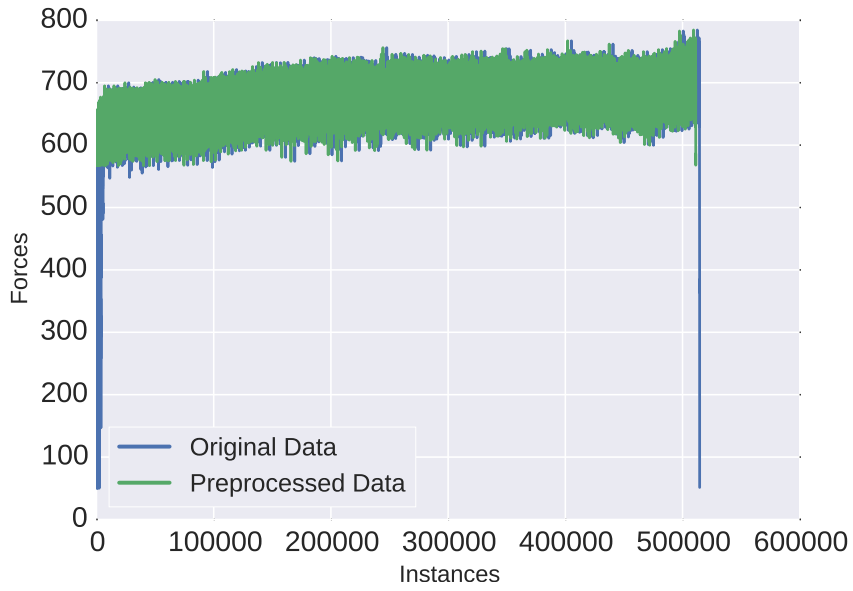

Fig. 2: Original data versus Filtered Data for Inconel 718, LGA, HPC, T2, pass 1.

3.2 Time series dimensionality reduction: PCA application

Principal component analysis (PCA) is a multivariate technique that analyzes a data table in which observations are described by several inter-correlated quantitative dependent variables. Its goal is to extract the important information from the table, to represent it as a set of new orthogonal variables called principal components, and to display the pattern of similarity of the observations and of the variables as points in maps [18]. This transformation is defined in such

a way that the first principal component has the largest possible variance and each succeeding component in turn has the highest variance possible under the constraint that it is orthogonal to the preceding components.

PCA identifies patterns in data and detects correlation between variables. The attempt to reduce dimensionality only makes sense when there is a strong correlation between variables. We are going to find the directions of maximum variance of the three forces considered and project them onto a smaller dimensional subspace while retaining most of the information.

Before starting with the analysis, we reduce the dimensionality of the time series using Piecewise Aggregate Approximation (PAA) [23]. This technique first divides the original time series into M equally sized frames and secondly computes the mean values for each frame. In this case we have used $M = 10000$. Since PCA yields a feature subspace that maximizes the variance along the axes it makes sense standardizing the data, although all variables are measured in Newtons they take different values. This analysis is made for all tests for Inconel 718, but as an example we are going to use Inconel 718, LGA, HPC, T2, pass 1. The reason to use this test as an example is that the projection onto the two principal components is delimitated by a box.

We are going to compute eigenvectors and eigenvalues of a covariance matrix. The eigenvectors (principal components), determine the directions of the new feature space and the eigenvalues determine their magnitude. The eigenvectors with the lowest eigenvalues bear the least information about the distribution of the data and those are the ones that can be dropped.

The covariance matrix, in this case a 3×3 dimension matrix (2), represents the covariance between two variables. The numbers that are in the main diagonal represent the variance of the variables, since they are standardized is 1. The correlation matrix can be seen as the covariance matrix of the standardized variables. As we can see, there is a strong correlation between F_x and F_y and significant correlation between F_x and F_z.

$$Cov = \begin{pmatrix} 1 & 0.91 & -0.6 \\ 0.91 & 1 & -0.47 \\ -0.6 & -0.47 & 1 \end{pmatrix} \tag{2}$$

A useful measure is the explained variance which can be calculated from the eigenvalues. The explained variance tells us how much information (variance) can be attributed to each of the principal components.

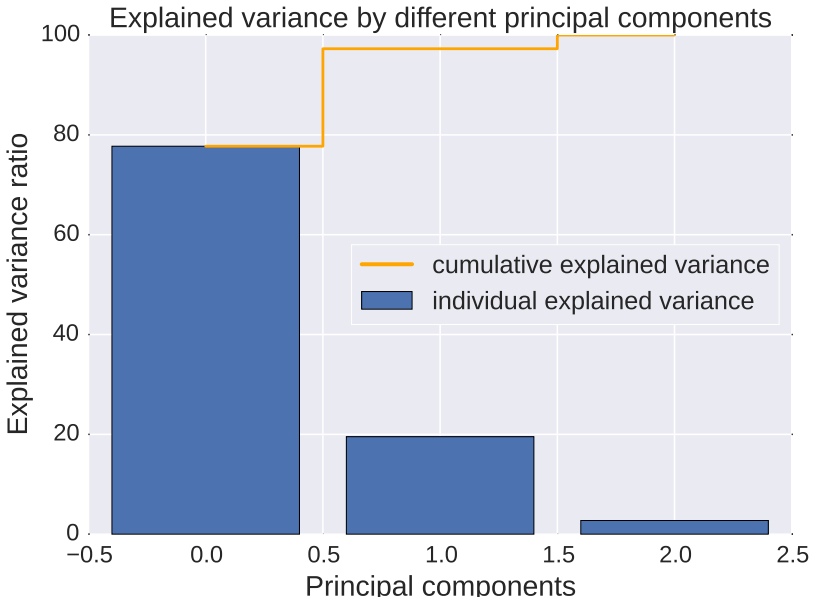

Fig. 3: Barchart that displays the eigenvalues associated with a component descending order versus the number of the components for Inconel 718, LGA, HPC, T2.

The plot (Fig. 3) clearly shows that with one principal component we can explain almost 80% of the variance which is a considerable quantity. The second principal component still bears some information while the third one can be dropped without losing too much information. Finally, we will use the 10000×2-dimensional projection matrix to transform our samples onto the new subspace.

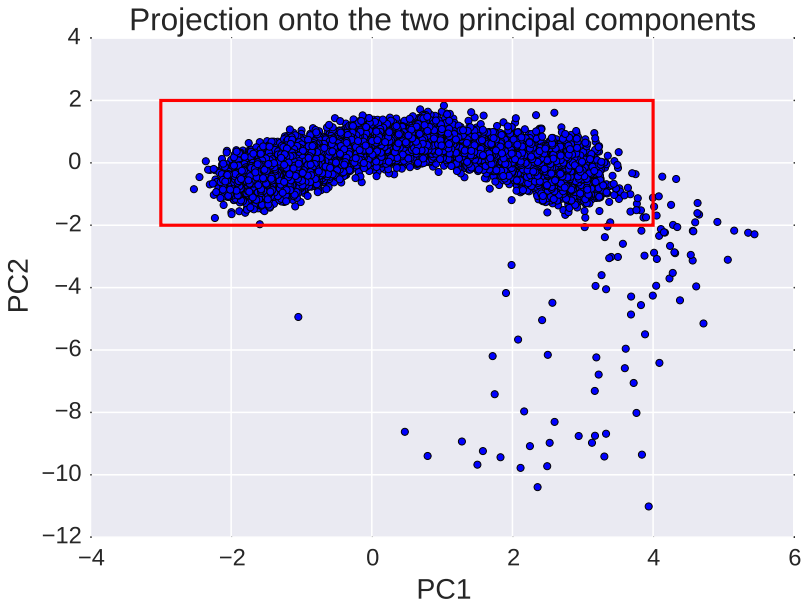

Fig. 4: Projection of the forces onto the new subspace for Inconel 718, LGA, HPC, T2, pass 1.

In the projection most of the points are grouped in the same region as we can observe in Fig. 4. In the next step we project the points that are out of the interval $(x, y) \in \{(-3, 4) \times (-2, 2)\}$ back onto the original representation in order to detect possible outliers.

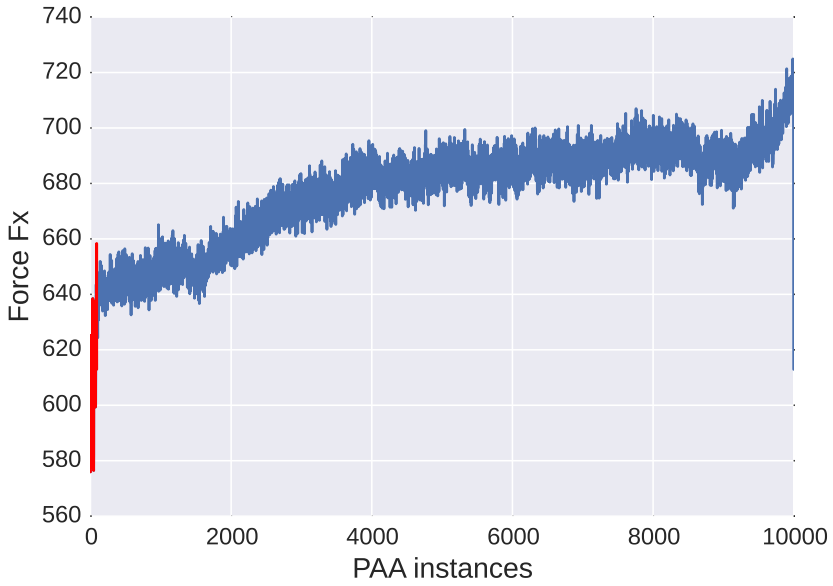

Fig. 5: Projection of the points that are out of the interval $(x, y) \in \{(-3, 4) \times (-2, 2)\}$ onto the original data for Inconel 718, LGA, HPC, T2, pass 1.

As we observe in Fig. 5. those points belong to the initial part of the pass when the force increases after a stop in the process.

In order to evaluate the capacity of PCA to capture characteristic patterns of the forces it was applied to all Inconel 718 tests for the first and last pass to see the evolution of the forces during the turning process. Table 8 shows the explained variance by two principal components with highest contribution to the explained variance. In all of the cases the explained variance is considerably large. For LGA and SGS states the explained variance is lower in the sixth pass than in the first pass though, for SGA and LGS the opposite occurs.

In general, there are not patterns that are repeated among tests that use the same lubrication or the same state. Fig. 6 presents two examples of shapes that have been repeated. In SGA HPC tests, the galaxy shape of the projected variance in pass 1, is repeated among the three tests that are available. For the sixth pass the pattern of the projected variance changes completely and it is repeated among the three tests.

State	Lubrication	Test number	Pass number	Explained variance percentage with two principal components
LGA	NORMAL	1	1	98.02
		1	6	93.99
		2	1	97.36
		2	6	95.58
	HPC	1	1	95.73
		1	6	86.50
		2	1	97.26
		2	6	90.98
SGA	NORMAL	1	1	91.54
		1	6	97.86
		2	1	76.30
		2	6	95.60
		3	1	92.33
		3	6	90.64
	HPC	1	1	81.38
		1	6	96.46
		2	1	89.39
		2	6	97.11
		3	1	83.20
		3	6	96.04
LGS	NORMAL	1	1	94.09
		1	6	98.21
		2	1	91.11
		2	6	96.88
SGS	NORMAL	1	1	93.79
		1	6	88.31
		2	1	93.85
		2	6	80.55

Table 8: Explained variance percentage by two principal components of the three forces involved in the turning of Inconel 718.

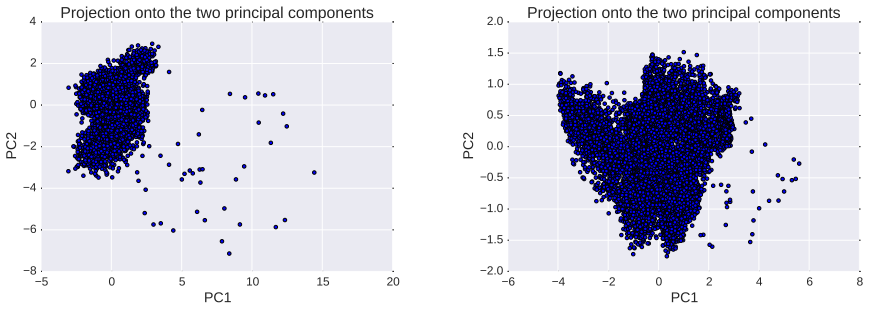

A

(a) Test 1, pass 1

B

(b) Test 1, pass 6

Fig. 6: Examples of shapes of the PCA representation of the forces (two components) that are repeated among the three available tests in Inconel 718, SGA, HPC.

Using exploratory data analysis we have first filtered the original data containing the measurements of the three forces. On the filtered signal, we have computed the principal components and identified that in all tests the explained variance percentage by the two most principal components is very high. We have identified, based on the PCA analysis and the visualization of the forces based on the most important principal components that, for one particular test, most of the points were delimited by a box. The values that were out of that box derive from the beginning of the pass (Fig. 5). In this particular example the PCA also serves to filter the noisy data belonging to the beginning of a test.

Apart from that, PCA analysis has revealed characteristic patterns in data among different passes, states and lubrications as it can be observed in Fig. 6. In the investigations [50] [49] [48] mentioned in Section 2, PCA was applied for feature extraction in different machining processes. In those investigations the models were constructed using the original variables and most important principal components and the performance of the predictive models in both cases were compared. In this thesis the mentioned technique has served to be aware of the differences that exist among different passes, states and lubrications but the three original variables (F_x, F_y, F_z) have been used in model construction. The main contribution of this section is the finding that for each state and lubrication there is the necessity to build a particular predictive model due to the differences that exist.

4 Flank Wear analysis

In this section we analyze the data to investigate the evolution of flank wear (amount and distribution) in the tool along the machining process. We also

analyze the influence that grain size and microhardness have on the flank wear. The descriptive analysis is a previous step towards wear prediction and we want to know how reliable are the variables flank wear mean and flank wear maximum to represent all flank wear measurements available from each test.

The influence of material state characteristics such as grain size and microhardness on wear has been the subject of previous research [36] [35]. In those investigations, mean flank wear and maximum notch wear were plotted and the relationship between wear and material characteristics was investigated; whereas we are going to apply statistical hypothesis testing approach to study that influence.

4.1 Analysis of the distribution of the flank wear in nine points

As explained in Section 1, in the experiment considered, the flank wear is measured in nine points for each pass in the material. Using these measurements, the maximum point and the mean are considered in the variables flank wear mean and flank wear maximum. In this section we will analyze the distribution of the flank wear in the nine points of the material where wear measurements were taken. For our analysis we will use descriptive statistics.

We will start with Inconel 718 material, SGS state, normal lubrication and test 4. Fig. 7 shows a picture of the tool used in the experiment where wear measurements are made for different points.

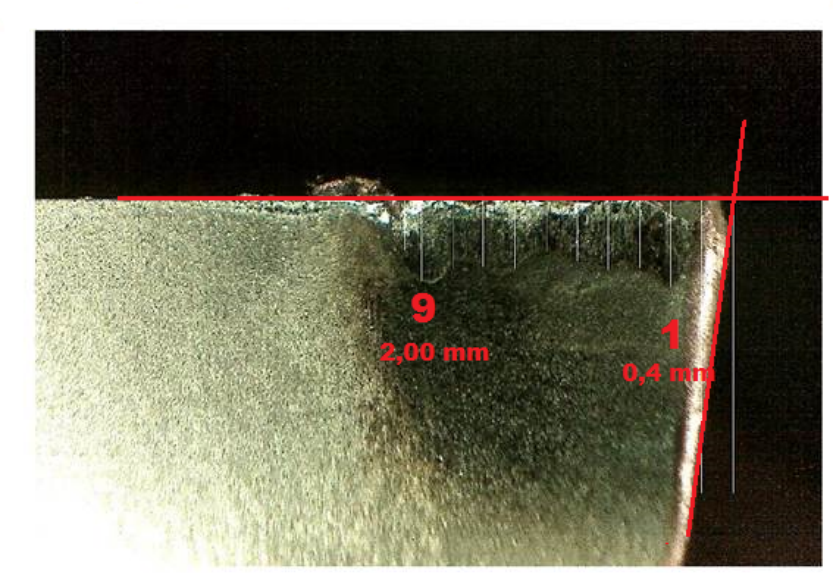

Fig. 7: Turning tool used in the experiments and points were flank wear measurements were taken. The flank wear values for the first and ninth points are shown in red.

Fig. 8 shows the evolution of the flank wear for each of the passes. In the figure, each symbol corresponds to one of the passes, the x axis represents the point number and the y axis represents the flank wear measurement.

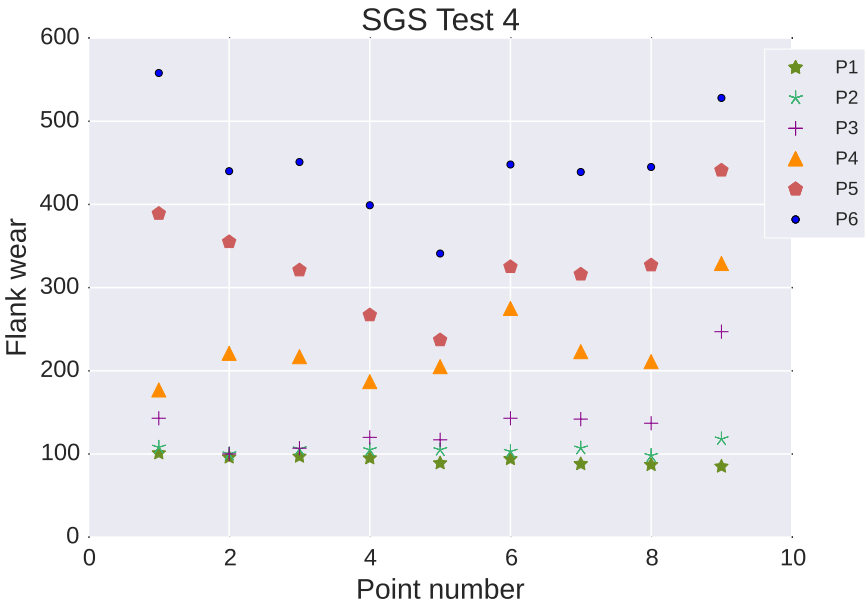

Fig. 8: Flank wear in nine points for the six passes in Inconel 718, SGS, NORMAL, T4.

For the last two passes the points that represent larger wear are the first and the ninth point. These points are located in the extremes of the edge of the tool. As the number of the passes increases, the dispersion of the points where the measurements were taken seem to be higher. We can confirm this fact looking to the evolution of the standard deviation in Table 9. For the six of passes the median and the mean of the sample are very similar so that we can conclude that the distributions of the ninth points are symmetric. The mean of a sample is representative if the values are close to the mean and in the case that there are not extreme values. In this case, it is appropriate to use the mean to represent the first two passes; for the rest of the cases the median will be more suitable.

Pass number	Mean	STD	Median	Maximum	Minimum
1	92.44	5.08	94	101	85
2	105.56	5.36	105	118	98
3	139.56	40.96	137	247	100
4	227.22	44.35	217	329	177
5	330.89	57.11	325	441	237
6	449.89	60.07	445	558	341

Table 9: Statistical parameters of the nine points where wear measurements were taken for each of the passes Inconel 718, SGS, NORMAL, T4.

Table 10 shows the statistical parameters of the nine points distributions for a different test of the same material, i.e. Inconel 718, LGS, NORMAL,T1. It can be observed in the table that the standard deviation is higher than in the previous table and its values increases with the number of passes. Until the fourth pass the wear is very similar for the six points and its values increase for the last two passes. For the point number seven the wear increases significantly from the first pass and so does for the rest of the passes (Fig. 9).

Pass number	Mean	STD	Median	Maximum	Minimum
1	110.33	46.16	82	189	72
2	147.89	67.50	106	264	95
3	164.00	70.05	118	295	111
4	194.67	64.33	172	314	104
5	245.67	72.04	227	384	144
6	270.00	80.44	253	434	157

Table 10: Statistical parameters of the nine points where wear measurements were taken for each of the passes Inconel 718, LGS, NORMAL, T1.

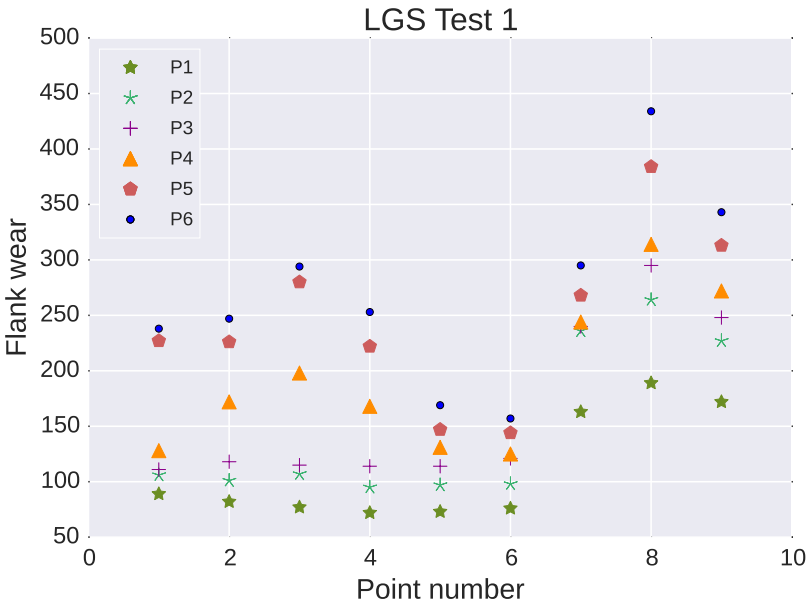

Fig. 9: Flank wear in nine points for the six passes in Inconel 718, LGS, NORMAL, T1.

In the case of SGA state test 1 there is a human error in one of the wear measurements. In the seventh point the wear decreases from pass 5 (229) to pass 6 (225). In order to deal with this type of errors, we will assume that the sixth point is a missing value. We will impute this value using information of the evolution of the wear in that seventh point and the increment on wear from pass 5 to pass 6 in the rest of the points. First, a linear regression model will be built for the seventh point and the five passes in order to predict the sixth one. Then, the average of the difference between passes five and six will be computed for the rest of the points. The final value will be the average of the increment of the two measurements. The use of linear regression is justified because the evolution of the points shows a linear trend in the plots.

The same method will be applied to state LGA test 1 because there is also a presence of human errors. In this case, there are errors in almost every point. Therefore, we will use linear regression with the first five passes in those points.

In the case of the state LGA, the higher wear achieved is in the point number one except for the fifth pass for which the highest flank wear is reached at the second point. For most of the points the increment of the wear starts being larger after the fourth pass. For the last point the values of some passes are missed (Fig. 10). In the case of the state SGA, the highest wear appears in the middle points (fifth and sixth). For the first of the passes there is an increment

between pass number five and pass number six that influences the consecutive passes. For the second and third passes the increment is in the pass number five (Fig. 11).

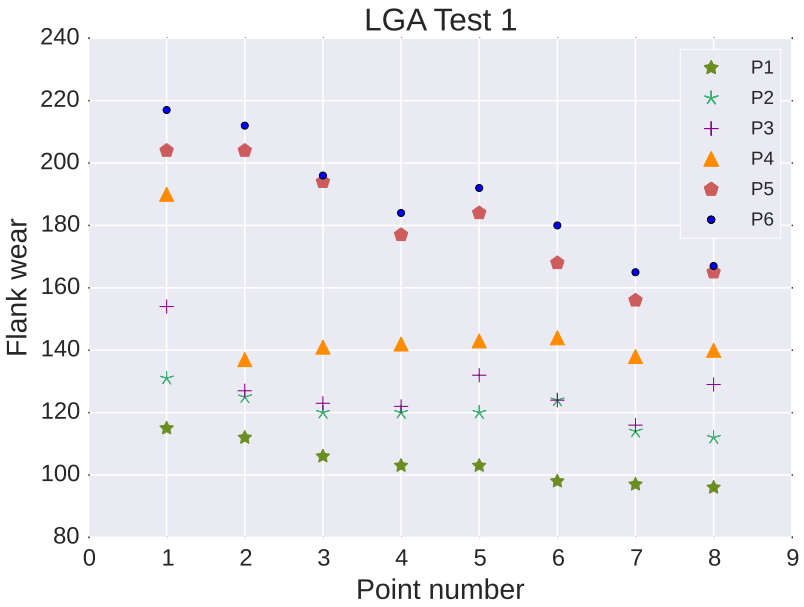

Fig. 10: Flank wear in nine points for the six passes in Inconel 718, LGA, NORMAL, T1.

Pass number	Mean	STD	Median	Maximum	Minimum
1	109.67	15.51	104	153	100
2	148.56	30.43	136	219	125
3	171.78	39.39	156	248	113
4	232.22	45.92	238	286	152
5	250.22	61.38	229	329	147
6	299.62	85.54	284	422	167

Table 11: Statistical parameters of the nine points where wear measurements were taken for each of the passes Inconel 718, SGA, NORMAL, T1.

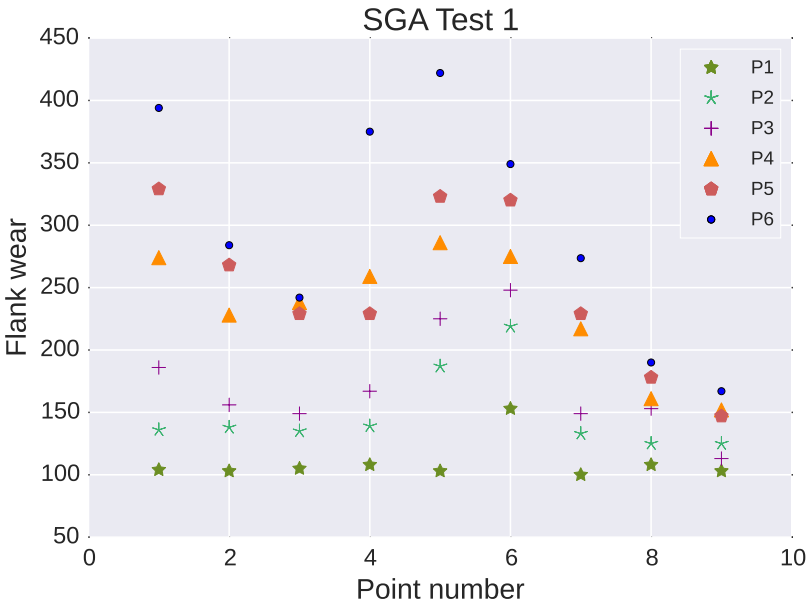

Fig. 11: Flank wear among nine points for the six passes in Inconel 718, SGA, NORMAL, T1

In the case of HPC lubrication, there is only data available in the states SGA and LGA. Fig. 12 and Fig.13 show the evolution of the flank wear for each of the passes.

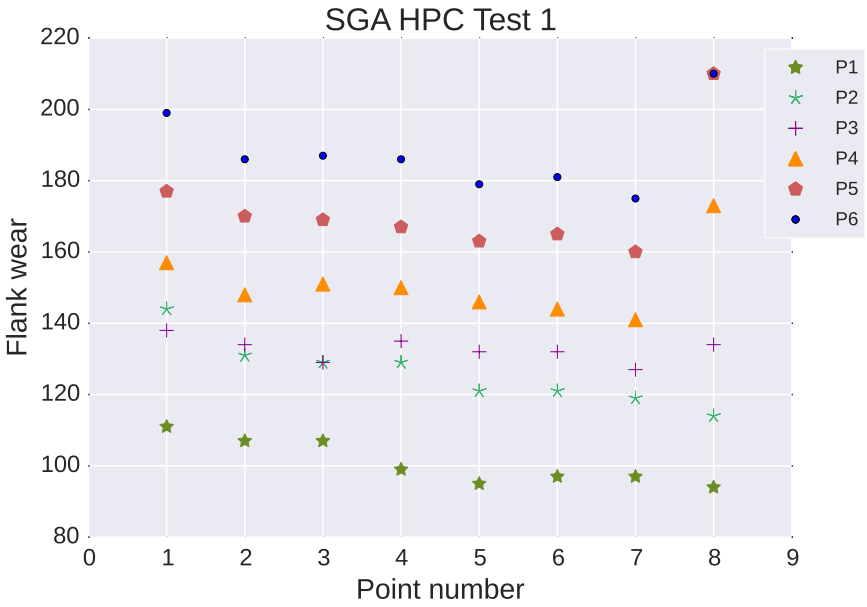

Fig. 12: Flank wear in eight points for the six passes in Inconel 718, SGA, HPC, T1.

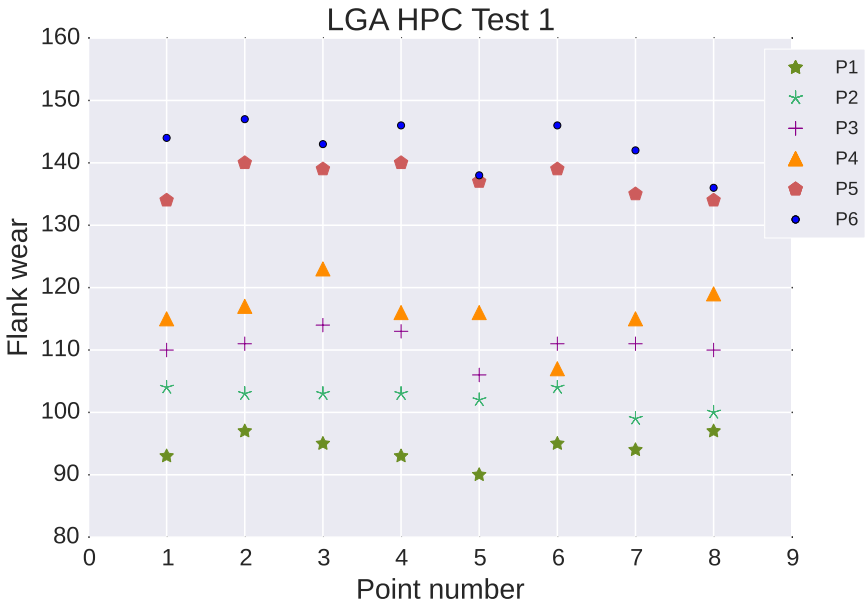

Fig. 13: Flank wear in eight points for the six passes in Inconel 718, LGA, HPC, T1.

As we can see in Fig. 12 and Fig.13 the distribution is more uniform among all the passes. The dispersion of the measurements is lower than in normal lubrication as standard deviation is quite low specially in the case of SGA (Table 12 and Table 13). One of the conclusions that can be extracted from the analysis of the figures is that when HPC lubrication is used, there are less differences between tests that have same characteristics (same state and lubrication).

Pass number	Mean	STD	Median	Maximum	Minimum
1	100.88	6.05	98	111	94
2	126.00	8.73	125	144	114
3	132.63	3.24	133	138	127
4	151.25	9.38	149	173	141
5	172.63	14.91	168	210	160
6	187.88	10.68	186	210	175

Table 12: Statistical parameters of the nine points where wear measurements were taken for each of the passes Inconel 718, SGA, NORMAL, T1.

Pass number	Mean	STD	Median	Maximum	Minimum
1	100.38	11.31	101	119	83
2	109.75	6.89	111	118	96
3	129.75	3.15	131	134	124
4	135.88	5.16	136.5	143	129
5	139.50	4.27	139	147	134
6	143.75	5.44	145	149	131

Table 13: Statistical parameters of the nine points where wear measurements were taken for each of the passes Inconel 718, LGA, NORMAL, T1.

This analysis has provided information about the distribution of the flank wear. Some human errors were found in the measurements and these values were imputed using linear regression. The reached conclusion is that the maximum value is less sensitive than the mean value when there are changes in the data and that the mean value is not a good descriptor of the general behavior of the points in all of the cases. We consider that the use of the maximum value of the flank wear measurements is a more appropriate choice for prediction of flank wear in these experiments.

4.2 Influence of grain size and microhardness: statistical hypothesis testing

There are several researches [36] [35] that have studied the effect and influence of grain size and hardness on wear. In those researches the mean flank wear and notch wear evolution were drawn to relate with the characteristics of the states (large/small grain size, solutioned/aged microhardness).

The objective of the study presented in this section is to determine the influence that the grain size and the microhardness of the superalloys have on the flank wear. For that purpose, on the one hand, we are going to compare states that have same grain size to analyze the effect of the microhardness. On the other hand, we will compare states that have the same microhardness to study the effect of the grain size.

The intent of a statistical test is to determine whether there is enough evidence to reject a conjecture or a hypothesis about the data been analyzed. The aim of this part of the analysis is to determine whether there are differences in the means of the populations; understanding the populations as measurements describing characteristics of the experiments in different tests. A hypothesis test attempts to refute a specific claim about a population parameter based on the sample data.

There are two main types of statistical test in literature: parametric tests and nonparametric tests. The sample's properties are going to determine which of

the two type of test is the best in each case. A parametric statistical test assumes that the data comes from a certain probability distribution and makes inferences about the parameters of the distribution. For example, in t-test or ANOVA there are three required conditions to be fulfilled: independence, normality and homoscedasticity [22]. The non parametric tests are used when the population cannot be assumed to be normally distributed.

We use the Wilcoxon signed-rank test, a non parametric statistical hypothesis test, because we have paired or dependent samples as the same nine points are tested using different states of the Inconel 718 material. In this hypothesis testing, the null hypothesis H_0, is that the two populations have same median; though the alternative hypothesis is that they have different medians. The strength of the evidence is supported by the p-value. Suppose the test statistic is W. The p-value is the probability of observing a test statistic as extreme as W, assuming the null hypothesis is true. If the p-value is less than the significance level ($\alpha = 0.05$), we reject the null hypothesis.

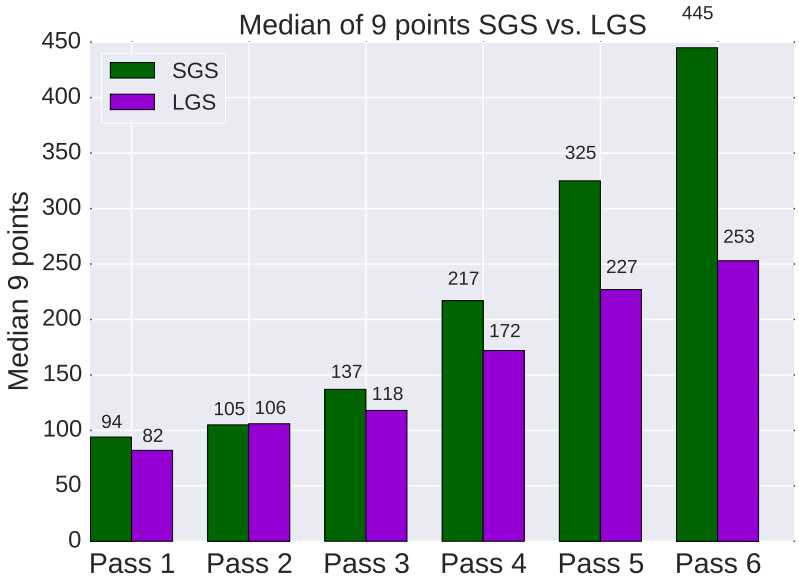

Fig. 14: Bar graph with the median of nine points for each of the six passes for Inconel 718 the states LGS and SGS

Fig. 14 shows the medians of the nine points of flank wear in both tests SGS and LGS. To analyze the influence of a different size of grain, large versus small, we will use the previous mentioned Wilcoxon signed-rank test.

Pass number	p-value
Pass 1	0.86
Pass 2	0.59
Pass 3	0.59
Pass 4	0.17
Pass 5	0.03
Pass 6	0.01

Table 14: The p-values obtained from the application of Wilcoxon signed-rank test to data obtained for Inconel 718 states SGS and LGS.

If we inspect Table 14, for the first 4 passes we do not reject the null hypothesis and we accept that the medians of the two populations are equal. However, For the last two passes, we reject the null hypothesis because the p-values are lower than the significance level 0.05. In Fig 15, the medians of the two populations are shown.

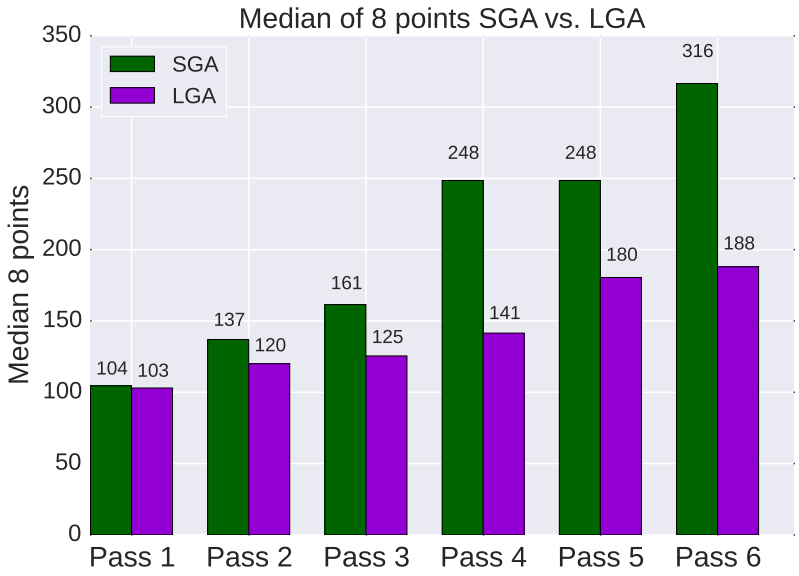

Fig. 15: Bar graph with the median of eight points for each of the six passes for Inconel 718 the states LGA and SGA.

If we compare the grain size but in the aged states we obtained the following p-values (Table 15).

Pass number	p-value
Pass 1	0.5
Pass 2	0.01
Pass 3	0.01
Pass 4	0.01
Pass 5	0.01
Pass 6	0.01

Table 15: The p-values obtained from the application of Wilcoxon signed-rank test to data obtained for Inconel 718 states SGA and LGA.

In this case, except for the first pass we assume that the medians for the two populations are different. The reached conclusion is that for the solutioned states the grain size influences only in the fifth and sixth pass while in aged states the grain size has an impact in almost every pass. That is to say that grain size has a major impact on wear in aged states than in solutioned states. Although, in an experiment carried out with Alloy 718 [36], similar flank wear mean was obtained for LGS and SGS and for LGA and SGA, in our investigations we have found that there are differences on the flank wear in the states LGA and SGA.

In the following part we will evaluate the influence of microhardness, aged and solutioned, in small and large grains. For that target, as we have done previously, the Wilcoxon signed-rank test will be used. In the case of LGA there are missing values for the ninth point in some of the passes. For that reason we will use eight points measurements.

Pass number	p-value
Pass 1	0.01
Pass 2	0.01
Pass 3	0.11
Pass 4	0.48
Pass 5	0.03
Pass 6	0.02

Table 16: The p-values obtained from the application of Wilcoxon signed-rank test to data obtained for Inconel 718 states SGS and SGA.

Pass number	p-value
Pass 1	0.59
Pass 2	0.67
Pass 3	0.67
Pass 4	0.2
Pass 5	0.12
Pass 6	0.07

Table 17: The p-values obtained from the application of Wilcoxon signed-rank test to data obtained for Inconel 718 states LGS and LGA.

The p-values returned by the non parametric statistical test are displayed in Tables 16 and 17. There is no significant difference in the medians of LGS and LGA states, whereas in SGS and SGA states, there is significant difference in the medians except for the third and fourth pass. The reached conclusion is that hardness has a higher impact on wear when small grain state is used comparing to the large grain.

There are some investigations [33] [17] whose aim is to study the difference between dry and high pressure lubrication in machining Inconel 718. To analyze the influence of the lubrication, we will compare samples from LGA and SGA states to see if there is a statistical difference in medians between normal and HPC lubrication. Table 18 and Table 19 show the p-values returned by the Wilcoxon signed rank test. As it was expected there are significant differences in the medians of the samples (except for the state SGA and pass 1).

Pass number	p-value
Pass 1	0.16
Pass 2	0.04
Pass 3	0.01
Pass 4	0.02
Pass 5	0.02
Pass 6	0.02

Table 18: The p-values obtained from the application of Wilcoxon signed-rank test to data obtained for Inconel 718 SGA state with normal and HPC lubrication.

Pass number	p-value
Pass 1	0.02
Pass 2	0.01
Pass 3	0.01
Pass 4	0.01
Pass 5	0.01
Pass 6	0.01

Table 19: The p-values obtained from the application of Wilcoxon signed-rank test to data obtained for Inconel 718 LGA state with normal and HPC lubrication.

In this section the effect that grain size and hardness have on wear has been studied using a statistical hypothesis testing approach. We have concluded that grain size has bigger influence on wear when the hardness is aged than when is solutioned. In the case of microhardness, it has impact on wear for small grains whereas it has not for large grains. In respect of lubrication, there was a significant difference in using normal or HPC lubrication.

The use of hypothesis testing, specially the ANOVA test, is quite extended in machining processes [38] [29] as we have mentioned in Section 2. In those investigations the ANOVA test was applied to identify influencing variables in the machining processes. The statistical test used in this thesis, has served to understand the differences that exist among the characteristics of the material and contribute to previous research with a statistical background. The significant difference in the distributions between normal and HPC lubrication suggests that their predictions should be treated in different ways.

5 Feature Selection

The main objective of this thesis is to generate a regression model to predict the flank wear using as input variables features extracted from the forces.

In this section, we will address the question of selecting a subset of relevant features to use in model construction. Feature subset selection is the process of identifying and removing as much irrelevant and redundant information as possible. This procedure reduces the dimensionality of the data, which in our case is necessary (it is impossible to deal with 500,000 points for further analysis). Although feature selection and feature extraction seem to be similar in fact they are different concepts [34]. In feature extraction, a new set of features is built from the original feature set that involves a transformation of the features. There are a variety of techniques for feature extraction including PCA, Independent Component Analysis (ICA) and matrix feature factorization. Feature selection

requires an understanding of what aspects of the database are relevant and important for the prediction that is going to be done [24].

The first features selected are some statistical parameters such as mean, variance and median of each of the forces and passes. For illustrative purposes the test used is Inconel 718, LGA, NORMAL, T2. It is very important to understand the relationship between variables to draw the right conclusion from a statistical analysis. The relationship between variables determines how the right conclusions are reached.

We study the relationship between features selected from the forces and the relative flank wear. We have considered the relative wear of each pass (the difference of consecutive wears), because there is high linear correlation between absolute wear and the time elapsed since the beginning of the experiment. We will use the Pearson's correlation coefficient which measures the linear correlation between two variables X and Y giving a value between -1 and 1 inclusive, where 1 corresponds to total positive correlation, 0 to no correlation and -1 is total negative correlation. The formula for the Pearson's correlation coefficient is:

$$r = r_{xy} = \frac{\sum x_i y_i - n\bar{x}\bar{y}}{(n-1)s_x s_y} \tag{3}$$

Where $X = \{x_1, ..., x_n\}$ and $Y = \{y_1, ..., y_n\}$ are two variables containing n values, $\bar{x}$ and $\bar{y}$ are the mean values of the variables and s_x and s_y standard deviation of the variables.

Table 20 shows the correlation between the different statistical descriptors extracted from the forces and the relative wear for the three forces. The numbers in bold are the ones that present a correlation coefficient higher than 0.6.

Forces	Mean	Minimum	Maximum	Variance	Median	Slope	Kurtosis
F_x	0.54	0.36	0.6	**0.76**	0.54	**0.69**	**-0.68**
F_y	0.57	0.53	0.35	**0.64**	0.58	**0.69**	-0.47
F_z	0.16	0.53	0.09	-0.11	0.22	0.45	-0.33

Table 20: Correlation between relative flank wear and statistical parameters of the forces for Inconel 718, LGA, NORMAL, T2.

The highest correlation between any of the measures derived from the forces is achieved for the variance. Also the slope exhibits a high correlation with the relative flank wear for the forces F_x and F_y. We conclude that when the force varies and fluctuates the flank wear increases. The only measurement that shows a negative correlation is the kurtosis.

Fig. 16 shows the visualization of the linear relationship between the variance of the force F_x for each pass and the relative flank wear. With the linear regression it is possible to predict the relative flank wear once the variance of the forces it is known. To carry out the goodness of fit of the statistical model more samples are needed.

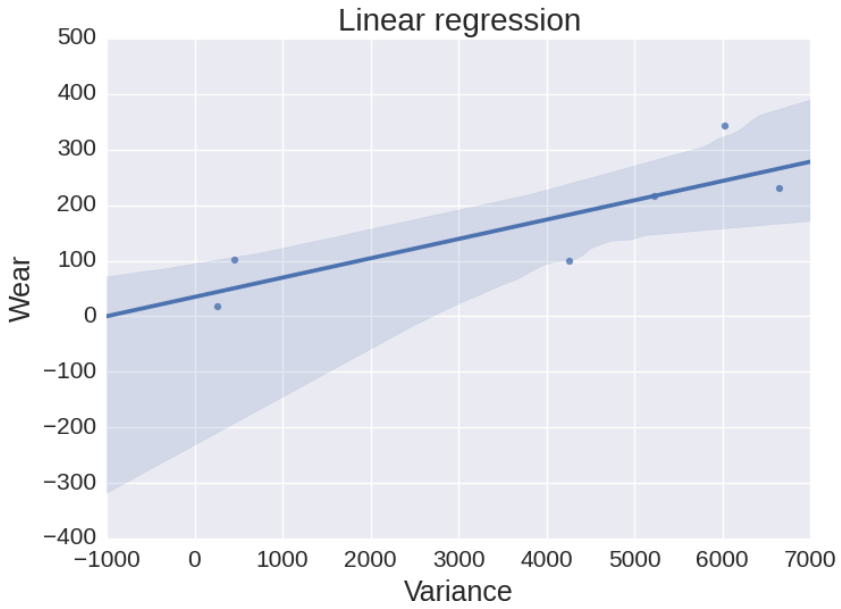

Fig. 16: The variance of F_x in each pass versus relative flank wear for Inconel 718, LGA, NORMAL, T2. The line corresponds to the lineal regression obtained from the data.

Identifying and analyzing peaks (or spikes) in a given time series is important in many applications [46]. Peaks indicate significant events such as a sudden decrease or increase and sharp rises. A data point in a time series is a *local peak* if it is a large locally maximum (or minimum) within a window. A point is considered a maximum peak if it has the maximal value, and was preceded (to the left) and followed (to the right) by a lower value. A similar strategy is used to detect peaks corresponding to local minimal values of the functions. In the analysis of the forces accomplished in this thesis, we have defined a way to detect the peaks. Our criterion to detect maxima and minima depends on a given parameter α and is defined as follows:

$$Maxima = \{x | x > Max \ \times \alpha\} \tag{4}$$

$$Minima = \begin{cases} x < Min \times (1+\alpha) & \text{if } Min > 0 \\ x < Min \times \alpha & \text{if } Min < 0 \end{cases} \tag{5}$$

Where, Max and Min are the maximum and minimum values of each of the forces for each test, and α is a constant value $0 < \alpha < 1$. We have chosen $\alpha = 0.8$. Fig. 17 and Fig.18 show the distribution of the number of peaks among the passes for forces F_x, F_y and F_z.

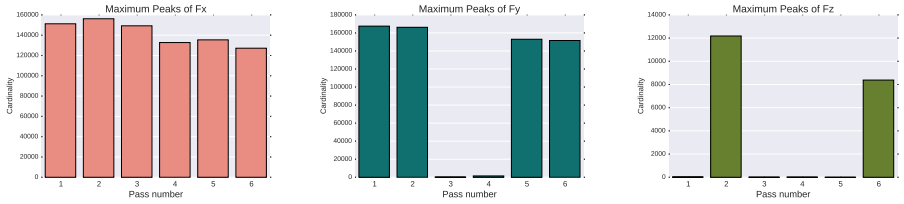

A B C

(a) F_x (b) F_y (c) F_z

Fig. 17: The number of maximum peaks for each force at each pass, Inconel 718, LGA, T2.

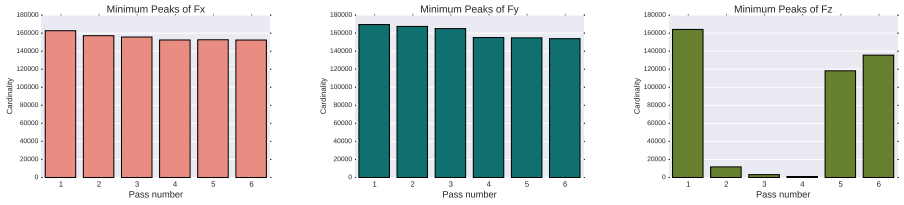

A B C

(a) F_x (b) F_y (c) F_z

Fig. 18: The number of minimum peaks for each force at each pass, Inconel 718, LGA, T2.

In some passes the number of peaks is really low in comparison with the others and that is because the singular points (maxima and minima) are less concentrated. It is the case of the force F_z (see Figures 17c and 18c) and the passes three and four from the maximum peaks of F_y (Figures 17b and 18b).

Once we have computed the local maximum and minimum values for each pass, we are going to consider some measurements derived from these values.

The measurements computed from the detected peaks are the following ones: mean, minimum, maximum, variance, median, kurtosis and number of peaks. Table 21 shows the correlation between the features and wear for Inconel 718, LGA, NORMAL, T2.

Forces	Mean	Minimum	Maximum	Variance	Median	Kurtosis	Cardinality
F_x max.peak	0.56	0.60	0.60	**0.94**	0.54	-0.51	-0.68
F_x min.peak	0.53	0.36	0.64	0.76	0.53	-0.69	-0.52
F_y max.peak	0.50	0.35	0.35	0.48	0.52	-0.04	-0.13
F_y min.peak	0.56	0.53	0.26	0.62	0.57	-0.55	**-0.66**
F_z max.peak	0.13	0.13	0.09	0.21	0.13	-0.53	-0.52
F_z min.peak	0.39	0.53	0.53	0.06	0.38	**-0.62**	0.39

Table 21: Pearson's correlation between statistical parameters of maximum and minimum peaks and relative maximum flank wear for Inconel 718, LGA, NORMAL, T2.

The bold numbers indicate the highest correlation coefficients for each of the forces. The highest Pearson's correlation coefficient corresponds to the variance of the maximum peaks of F_x, followed by the number of minimum peaks of F_y. The pointedness of the distribution of the minimum peaks of F_z also has a high correlation with the relative flank wear.

As some features correspond to statistical parameters of the peaks distributions, in Fig. 19, Fig. 20 and Fig. 21 the distribution of maximum and minimum peaks are shown. These peaks distributions corresponds to Inconel 718, LGA, NORMAL, T2 test and are presented for illustrative purposes.

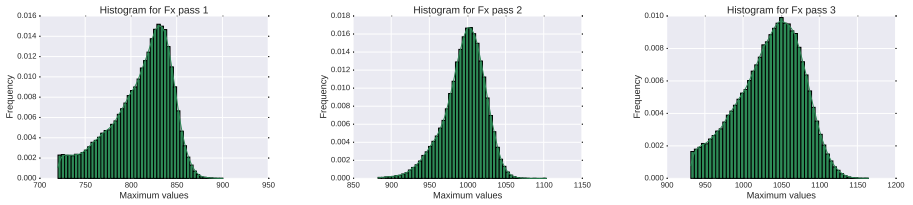

A

(a) Maxima, Pass 1

B

(b) Maxima, Pass 2

C

(c) Maxima, Pass 3

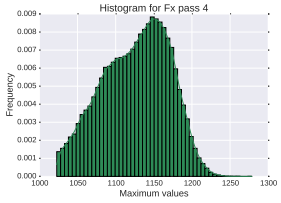

D

(d) Maxima, Pass 4

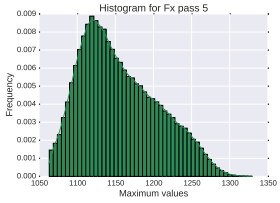

E

(e) Maxima, Pass 5

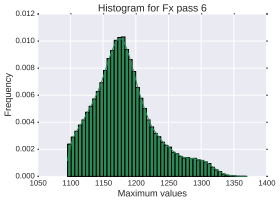

F

(f) Maxima, Pass 6

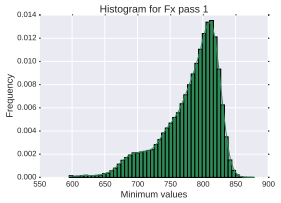

G

(g) Minima, Pass 1

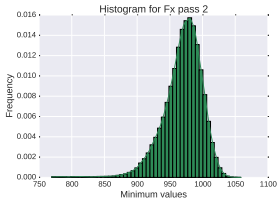

H

(h) Minima, Pass 2

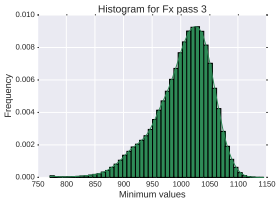

I

(i) Minima, Pass 3

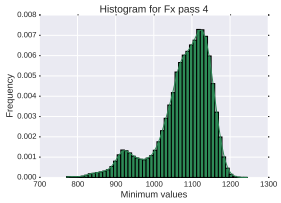

J

(j) Minima, Pass 4

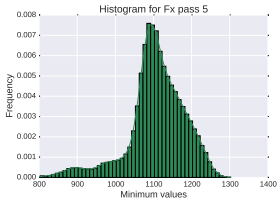

K

(k) Minima, Pass 5

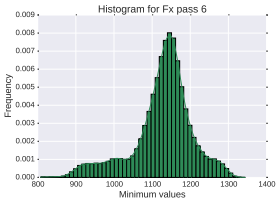

L

(l) Minima, Pass 6

Fig. 19: The distribution of maximum and minimum peaks of F_x, Inconel 718, LGA, T2.

The distribution of the points support a very informative dynamic view of how forces changes along the different passes of the experiment. We observe that some data represented in the figures follow the normal distribution. Another finding from the analysis of the figures is that the maximum values of F_x increase from one pass to the next one and the same occurs with the minimum values.

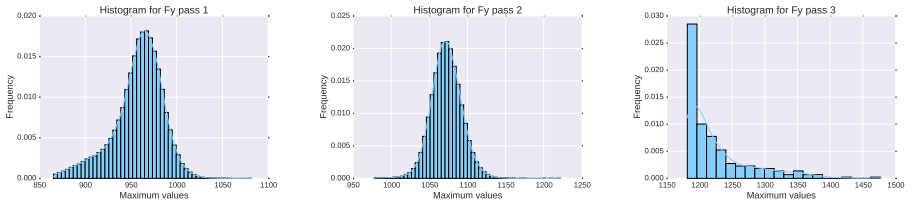

A

(a) Maxima, Pass 1

B

(b) Maxima, Pass 2

C

(c) Maxima, Pass 3

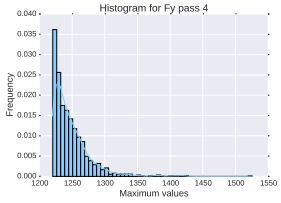

D

(d) Maxima, Pass 4

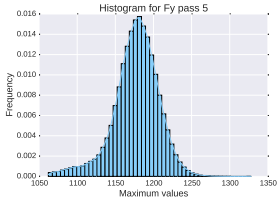

E

(e) Maxima, Pass 5

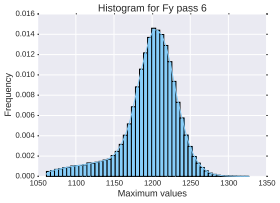

F

(f) Maxima, Pass 6

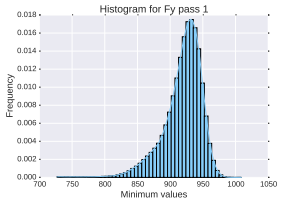

G

(g) Minima, Pass 1

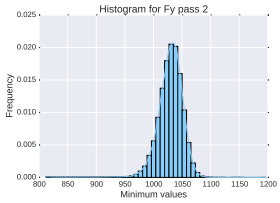

H

(h) Minima, Pass 2

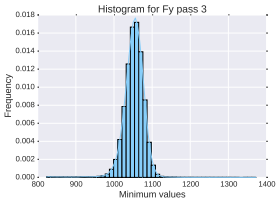

I

(i) Minima, Pass 3

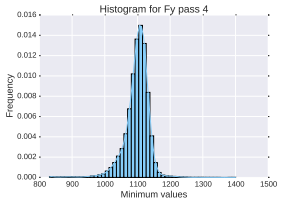

J

(j) Minima, Pass 4

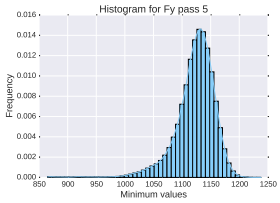

K

(k) Minima, Pass 5

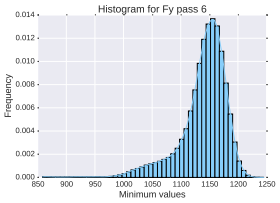

L

(l) Minima, Pass 6

Fig. 20: The distribution of maximum and minimum peaks of F_y, Inconel 718, LGA, T2.

In the case of F_y, the distributions are more concentrated around a number of points than the distributions of F_x. The values of maximum peaks of F_y increase until pass 4 but decrease from pass 4 to 5 and remain constant from pass 5 to 6. In passes three and four of the maximum peaks, the shape of the distribution is quite different and there are less peaks than in other cases.

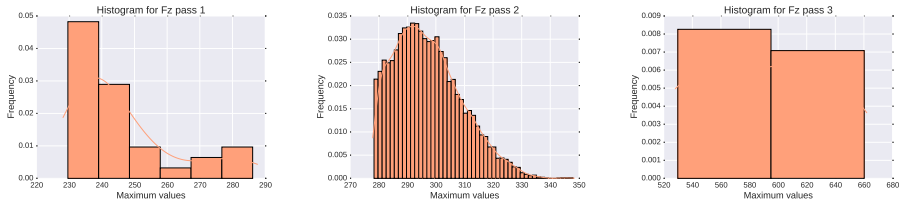

A

(a) Maxima, Pass 1

B

(b) Maxima, Pass 2

C

(c) Maxima, Pass 3

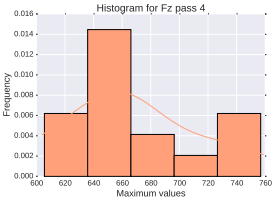

D

(d) Maxima, Pass 4

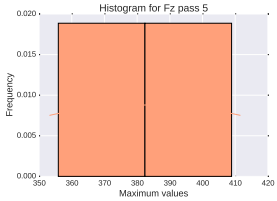

E

(e) Maxima, Pass 5

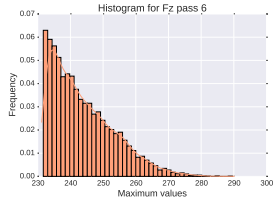

F

(f) Maxima, Pass 6

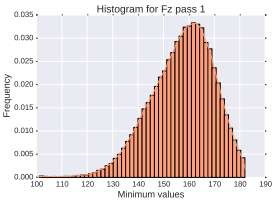

G

(g) Minima, Pass 1

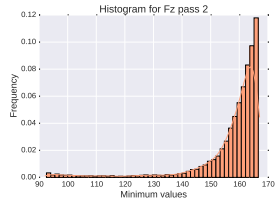

H

(h) Minima, Pass 2

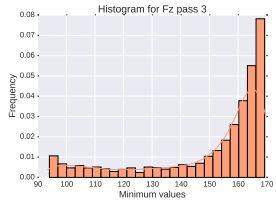

I

(i) Minima, Pass 3

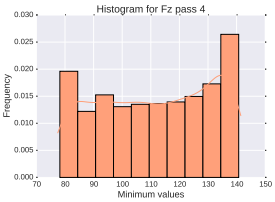

J

(j) Minima, Pass 4

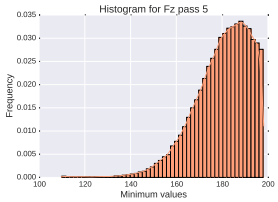

K

(k) Minima, Pass 5

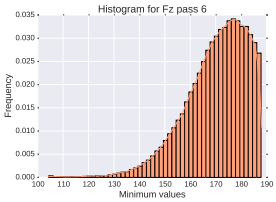

L

(l) Minima, Pass 6

Fig. 21: The distribution of maximum and minimum peaks of F_z, Inconel 718, LGA, T2.

In the case of F_z the distributions of the peaks are quite different comparing to F_x and F_y. The cuantity of the peaks changes significantly from one pass to other. As it has occurred to F_y, the values of maximum peaks increase until pass four and decrease for passes five and six.

In Table 22, we present the 21 features computed for the force F_x that will be used as a basis for predicting the flank wear, as explained in the next chapter. The table shows the indexes of the variables from 0 to 20. Each variable is the application of a statistical measure (e.g. Mean) one of the three parameters extracted from force F_x: 1) Raw F_x measurements, 2) Maximum Peaks, 3) Minimum Peaks. The same features are considered also for F_y and F_z.

Statistical Parameters	F_x	Maximum Peaks	Minimum Peaks
Mean	0	7	8
Minimum	1	9	10
Maximum	2	11	12
Variance	3	13	14
Median	4	15	16
Slope	5	-	-
Kurtosis	6	17	18
Cardinality	-	19	20

Table 22: Summary table of the selected features for the force F_x.

The prediction of the tool wear is a complex task due to the number of factors that influence the process of machining. The analysis presented in this chapter has illustrated how the behavior of the forces is related to the flank wear. The features derived from the forces will serve as an input features for the models presented in the next chapter.

6 Wear Prediction

As mentioned in Section 1, knowledge about the tool wear process and the capability to predict tool wear are of great importance. Tool wear is one of the most important topics in the cutting field. Analytical models able to forecast the tool wear with satisfactory accuracy, can give to the companies valid instruments to optimize the cutting processes [4]. Predictive performance models could be effectively used for machining processes reducing and/or eliminating trial and error approaches [3].

In this section we will investigate different strategies for predicting the maximum flank wear using the features selected in the previous section. For that purpose some regressors will be used and validated for each of the states for Inconel 718.

We will start with Inconel material LGA state and normal lubrication, for which two tests (T1 and T2) are available. We have in total 12 samples (each test consists on 6 passes) and 21 features for each of the forces F_x, F_y and F_z.

A predictive model is made up of a number of *predictors* which are variables that influence future behavior or results. In predictive modeling, data is collected, a statistical model is formulated, predictions are made and the model is validated. One of the most used predictive modeling is linear regression which models the relationship between a scalar dependent variable y and one or more explanatory variables X [47].

To define the train and test sets we will use the leave-one-out cross-validation technique. In k-fold cross-validation the dataset $\mathcal{D}$ is randomly split into k subsets (the folds) $\mathcal{D}_1, \mathcal{D}_2, ..., \mathcal{D}_k$ of approximately equal size. Sets are used to train and test k times; each time $t \in \{1, 2, ..., k\}$ it is trained on $\mathcal{D} \backslash \mathcal{D}_t$ and tested on $\mathcal{D}_t$. Leave-one-out corresponds to n-fold cross-validation [28].

Mean squared error (MSE) has been used to compute the prediction error produced by the different models. MSE is a measure of how close a fitted value is to the data point. It measures the average of the squares of the errors (the difference between observed and fitted values) [47]. If $\hat{y}$ is a vector of n predictions and y the vector of observed values, then MSE is calculated in the following way:

$$MSE = \frac{1}{n} \sum_{i=1}^{n} (\hat{y}_i - y_i)^2 \tag{6}$$

6.1 Applied regression methods

The following regressors have been applied to the features in order to predict the flank wear:

- Linear Regression
- Decision Tree Regressor
- Random Forest Regressor
- Adaptive Boosting Regressor
- Boostrap Aggregating Regressor
- k Nearest Neighbours Regressor
- Gradient Boosting Regressor

Decision Tree Regressor, having its origin name in machine learning theory, is an efficient tool for the solution of classification and regression problems [62]. The decision tree is based on a multistage or hierarchical decision scheme or a tree like structure. The tree is composed of a root node (containing all data), a set of internal nodes (splits) and a set of terminal nodes (leaves). In a decision tree approach, features of data are predictor variables whereas the class to be mapped is referred to as the target variable [8]. When the target variable is discrete it is known as a decision tree classification. In contrast, when the target variables are continuous it is known as decision tree regression. The decision tree

approach is built upon the assumption that the relationship between features and target objects is either linear or non-linear [62].

The random forest is an ensemble learning approach that can be used for classification or regression. The random forest starts with a standard machine learning technique called decision tree. In a decision tree, an input is introduced at the top and as it crosses down the tree the data gets lifted into smaller sets. The random forest takes this notion by combining trees with the notion of an ensemble. When a new input is entered into the system, it is run down all of the trees. The result may either be an average or weighted average of all of the terminal nodes that are reached [7].

Boosting is a general method for improving the accuracy of any given learning algorithm [45]. AdaBoost regressor (short form of Adaptive Boosting) is a machine learning meta-algorithm that can be used with other learning algorithms to improve their performance. The output of those learning algorithms is combined into a weighted sum that performs the final output, the learning algorithms are lightly modified in favor of the samples that present big errors. The base learning algorithm used by Adaptive Boostig Regressor we employ is the decision tree regressor [39].

Bootstrap aggregating (bagging), is an ensemble learning approach to improve accuracy and performance of other learning algorithms used for regression. Bagging was proposed to reduce prediction error of learning algorithms. Given a model, bagging applies the learning algorithm to each bootstrap sample and finally it aggregates the computed models by the mean (regression) or voting (classification) [40].

k nearest neighbours is a non-parametric method used for classification in machine learning. The approach is built on the idea of classifying a testing point, based on a fixed number k of its closest neigbours in the feature space. When used for regression, kNN estimates the response of testing point $\mathbf{x}_t$, as the average of the values of its k nearest neighbours [25]. A common distance metric used for continuous variables is the Euclidean distance.

Gradient boosting is a machine learning algorithm for classification and regression that makes prediction based on other learning algorithms typically using decision trees. Gradient boosting allows differentiable loss functions (functions that map values representing the cost associated to the events). Gradient boosting constructs additive regression models by sequentially fitting a base learner to current pseudo-residuals by least squares at each iteration. The pseudo-residuals are the gradient of the loss functional being minimized [21].

6.2 Implementation of the algorithms

Scikit-learn, a machine learning Python library was used to generate these regression models [39]. Table 23 and Table 24 present the parameters used by the regression algorithms. They have been included for the sake of reproducibility

of the experiments. A detailed explanation of the meaning of the parameters and their role in the behavior of the regression algorithm can be obtained from Scikit-learned documentation. [3]

Regressor	Parameter	Parameter value
Random Forest	n_estimators	100
	criterion	MSE
	max_features	n_features
	max_depth	None
	min_samples_split	2
	min_samples_leaf	1
	min_weight_fraction_leaf	0
	max_leaf_nodes	None
	bootstrap	True
	Oob-score	False
	n_jobs	1
	random-state	None
	verbose	0
	warm-start	False
Linear Regression	fit_intercept	True
	normalize	False
	copy_X	True
	n_jobs	1
Adaptive Boosting Regressor	base_estimator	DecisionTreeRegressor
	n_estimators	100
	learning_rate	1
	loss	Linear
	random_state	None

Table 23: Parameters used by the Random Forest Regressor, Linear Regression and Adaptive Boosting Regressor.

[3] `http://scikit-learn.org/stable/index.html`

Regressor	Parameter	Parameter value
Bootstrap Aggregating Regressor	base_estimator	None
	n_estimators	100
	max_samples	1
	max_features	1
	bootstrap	True
	bootstrap features	True
	Oob_score	False
	warm_start	False
	n_jobs	1
	verbose	None
	random_state	0
K Neighbours Regressor	n_neighbours	5
	weights	uniform
	algorithm	auto
	leaf_size	30
	p	2
	metric	minkowski
	metric_params	None
	n_jobs	1
Decision Tree Regressor	criterion	MSE
	sppliter	best
	max_depth	None
	min_samples_split	2
	min_samples_leaf	1
	min_weight_fraction_leaf	0.0
	max_features	None
	random_state	None
	max_leaf_nodes	None
	presort	False
Gradient Boosting Regressor	loss	least square
	learning_rate	0.1
	n_estimators	100
	subsample	1
	min_samples_split	2
	min_samples_leaf	1
	min_weight_fraction_leaf	0
	max_depth	3
	init	None
	random_state	None
	max_features	None
	alpha	0.9
	verbose	0
	max_leaf_nodes	None
	warm_start	False
	presort	auto

Table 24: Parameters used by the Boostrap Aggregating Regressor, kNN Regressor, Decision Tree Regressor and Gradient Boosting Regressor.

The programs to extract, filter, analyze and link the Scikit-learn modules with the original data of the experiments were implemented in Python.

6.3 Large Grain Aged

In this section the prediction of the flank wear will be carried out for large grain and aged microhardness state for the two lubrications that are available: normal and high pressure. To perform that predictions the regression methods presented in Section 6.1 will be used. The validation of the predictions will be made by using MSE measurement.

6.3.1 Normal Lubrication

The regression methods mentioned in Section 6.1 have been applied to LGA state normal lubrication test 1 and test 2. Data for regression problems is set up by organizing into two matrices, the input matrix and the target matrix. The input matrix is made of the 63 features (columns) and the 12 test cases (rows). The target matrix contains the maximum flank wear measurements.

The MSE measure allows us to determine which of the applied methods produces the best prediction. The MSE values computed from the outputs of these methods are shown in Table 25. One first observation from the analysis of the table is that they are quite large in all of the cases. The algorithm for which the lowest error has been achieved is the Gradient Boosting Regressor.

Another remarkable finding is that linear regression is the worst method. This is relevant because Linear Regression is perhaps the most common algorithm applied for these problems. It also supports the convenience of investigating the performance of other regression approaches as done in this thesis.

Regressors	MSE
Random Forests	965.79
Linear Regression	4743.36
Ada Boost	1213.27
k Neighbours	993.84
Bagging	3576.08
Decision Tree	1935.34
Gradient Boosting	875.06

Table 25: Mean squared error in prediction of the flank wear for each of the regressors, Inconel 718, LGA, NORMAL.

Real maximum flank wear and predicted maximum flank wear for all applied regression methods are shown in Fig. 22. The first six values correspond to test 1 and the consecutive six values to test 2.

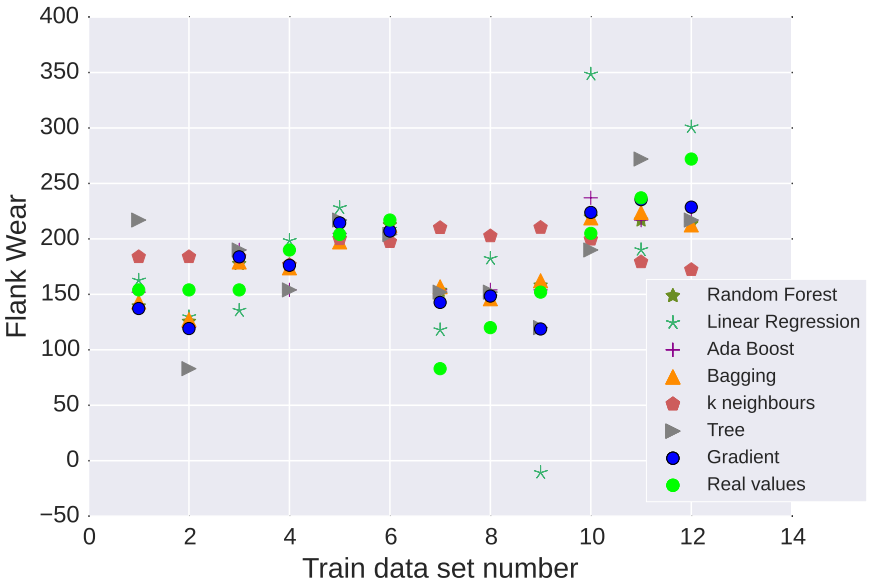

Fig. 22: Real and predicted values for flank wear using different regressors, Inconel 718, LGA, NORMAL. The first six values correspond to test 1 and the consecutive six values to test 2.

It can be observed in Fig. 22 that the flank wear increases from one pass to other (or it remains constant) but never decreases. The regression methods applied are not able to learn this tendency. Also, it can be appreciated that the k neighbours regressor is quite uniform among all the passes and linear regression does not perform well as for the ninth point the predicted value takes a negative number.

In order to have a clearer vision of the prediction we will represent real values versus predicted values for the Gradient Boosting Regressor as it has the lowest MSE value. In Fig. 23, real and predicted values are shown for the Gradient Boosting Regressor.

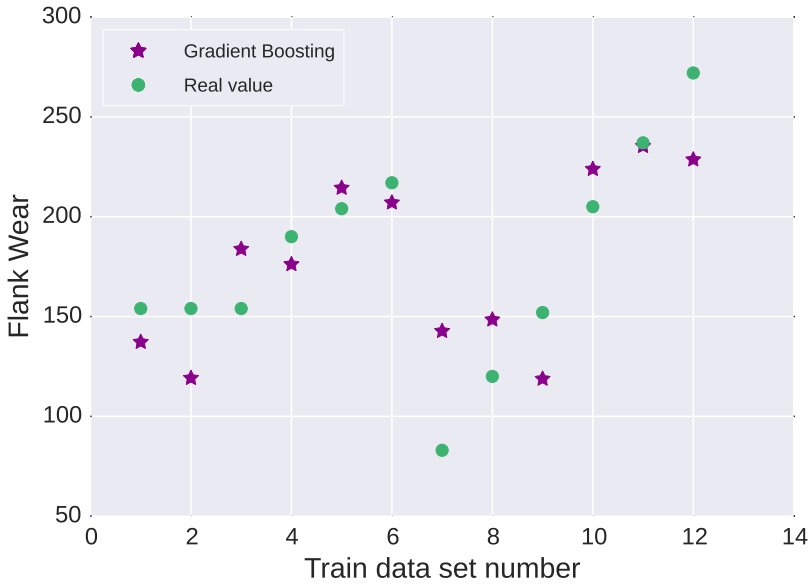

Fig. 23: Real and predicted values using Gradient Boosting Regressor for Inconel 718, LGA, NORMAL.

In Fig. 23, the first six values from test 1 seem to be more precisely predicted than values from test 2. As mentioned before the model is not able to learn the increasing tendency of the flank wear for one pass to other. The flank wear becomes critical in $300\mu m$ but in this case the critical value is not achieved. For that reason the prediction of the points that correspond to the last passes is very relevant. For the last pass, in both of the tests, the predicted value is lower than the real value.

It would be interesting to improve the prediction performance and for that purpose feature importances computed by Random Forest Regressor will be used. Firstly, the data from the first test (including the six observations) will be utilized to learn the prediction and compute feature importance and then the Random Forest Regressor will be applied and validated with the second test using the reduced feature subspace. As we have used leave-one-out to define training and testing tests we will obtain six estimations of the feature importance (one vector with the feature importance estimation for each of the six leave-one-out model learning steps) that provide us their importance. For each feature, the predicted feature importance will be the mean of the six estimations associated to each model learned.

In Fig. 24, the 63 features and the importance given by the regressor are shown. The threshold used to define the reduced feature subspace was $\lambda = 0.02$.

That it is to say that we will retain the features that have importance value higher than 0.02.

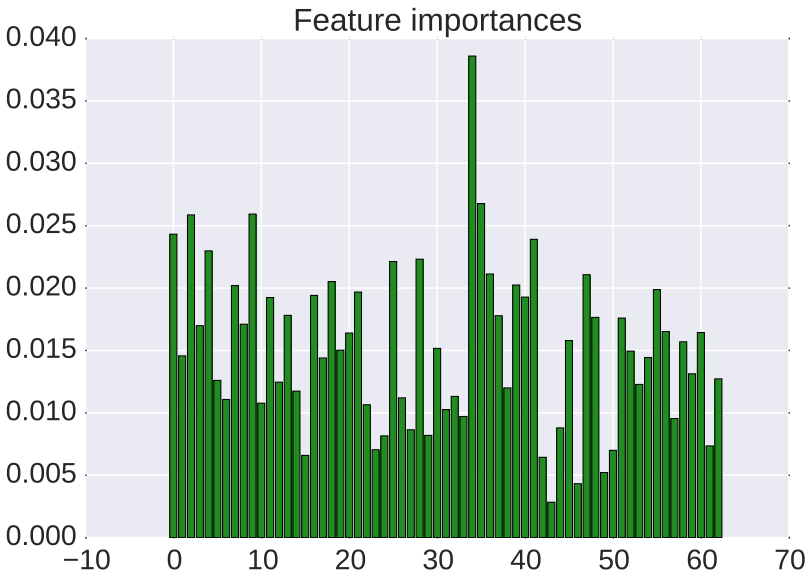

Fig. 24: Barplot of feature importance given by the Random Forest Regressor for Inconel 718, LGA, NORMAL.

The regression methods will be applied but with the reduced feature subspace (in this case 14 features). In Table 26, the chosen features are shown.

Feature number	Feature name	Related force	Feature importance
34	variance of maximum peaks	F_y	0.038597
35	variance of minimum peaks	F_y	0.026775
9	minimum of maximum peaks	F_x	0.025934
2	maximum	F_x	0.025866
0	mean	F_x	0.024323
41	number of minimum peaks	F_y	0.023912
4	median	F_x	0.022984
28	mean of maximum peaks	F_y	0.022320
25	median	F_y	0.022133
36	median of maximum peaks	F_x	0.021130
47	slope	F_z	0.021077
18	kurtosis of minimum peaks	F_x	0.020521
39	kurtosis of minimum peaks	F_y	0.020248
7	mean of maximum peaks	F_x	0.020198

Table 26: The most important features selected by Random Forest Regressor for Inconel, LGA, NORMAL.

An analysis of Table 26 reveals that half of the features correspond to the force F_x, though the first two most important features are related to F_y. There are some statistical parameters that are repeated as the variance and the kurtosis. The distance of the peaks from the mean (variance) and the pointedness of the distribution seem to be good predictors of the flank wear. There are more features related to the distribution of the peaks than parameters that describe general performance of the forces.

Fig. 25 shows the predicted and real values of the flank wear using Gradient Boosting Regressor with the 14 features learnt from the first test.

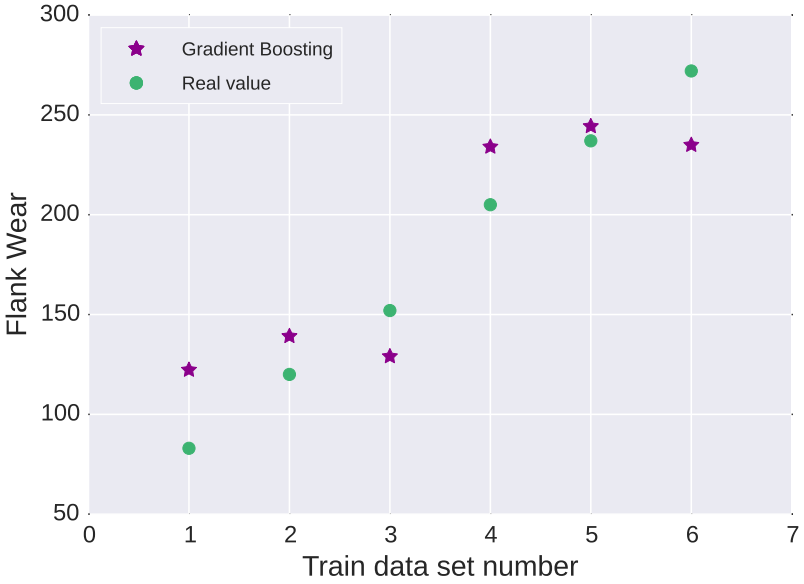

Fig. 25: Real and predicted flank wear using Gradient Boosting Regressor (14 features) for Inconel 718, LGA, NORMAL.

In Fig. 25, there is always an increment of the maximum flank wear as mentioned before though, the improved predictor is not able to learn that tendency. For the pass number three and six, the flank wear achieved is lower than the previous one. For the pass number 5 the achieved prediction is similar to the real value.

Although we compute the feature importance with Random Forest Regressor, once the feature subspace has been changed; the Gradient Boosting regressor performs better that the mentioned regressor. The MSE obtained is 784.45 lower than the one we had before.

6.3.2 High Pressure Lubrication

In this section, a study similar to the one presented in the previous section will be carried out for Large Grain Aged state using HPC lubrication. For that purpose the tests used are, Inconel 718, LGA, HPC, T1 and T2. Table 27 shows the MSE values obtained for all the applied regressor methods.

Regressors	MSE
Random Forests	109.61
Linear Regression	60.20
Ada Boost	144.00
k Neighbours	121.46
Bagging	267.93
Decision Tree	39.58
Gradient Boosting	74.33

Table 27: Mean squared error in prediction of the flank wear for each of the regressors, Inconel 718, LGA, HPC.

An analysis of Table 27 reveals that the MSE values are quite lower than the ones obtained for normal lubrication. The lowest one is for the Decision Tree Regressor. In Fig. 26 the predicted versus real values are plotted for the mentioned regressor.

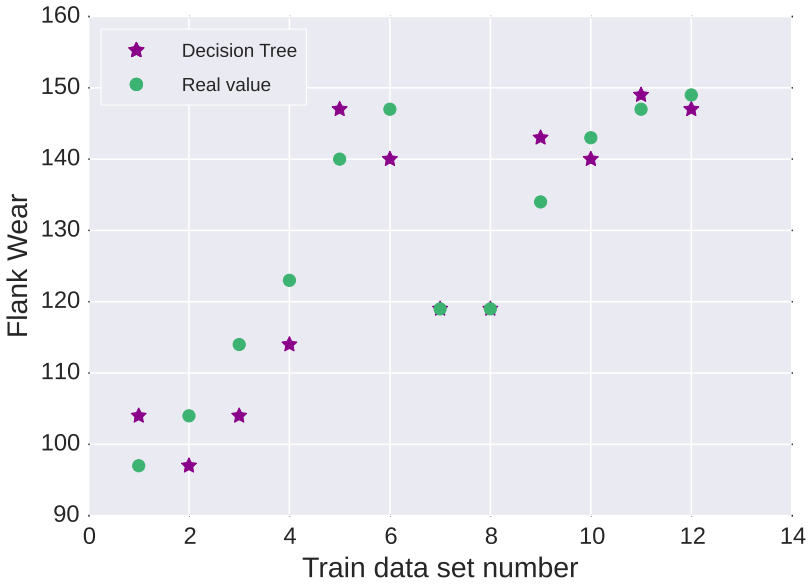

Fig. 26: Predicted and real values of flank wear using Decision Tree Regressor, Inconel 718, LGA, HPC.

If we compare Fig. 25, that shows the results corresponding to normal lubrication, with Fig. 26, it can be observed that the accuracy achieved for HPC is

considerably better. As it has occurred with normal lubrication, the prediction for the sixth pass is lower than the real value. The predictions for the first two passes for the test 2 are remarkably accurate.

As it has been done for normal lubrication, Random Forest Regressor is going to be used to estimate the feature importance and evaluate if there is an improvement in terms of MSE. In Fig. 27, importance values for the 63 features are shown. $\lambda = 0.02$ is used to choose the reduced feature subspace.

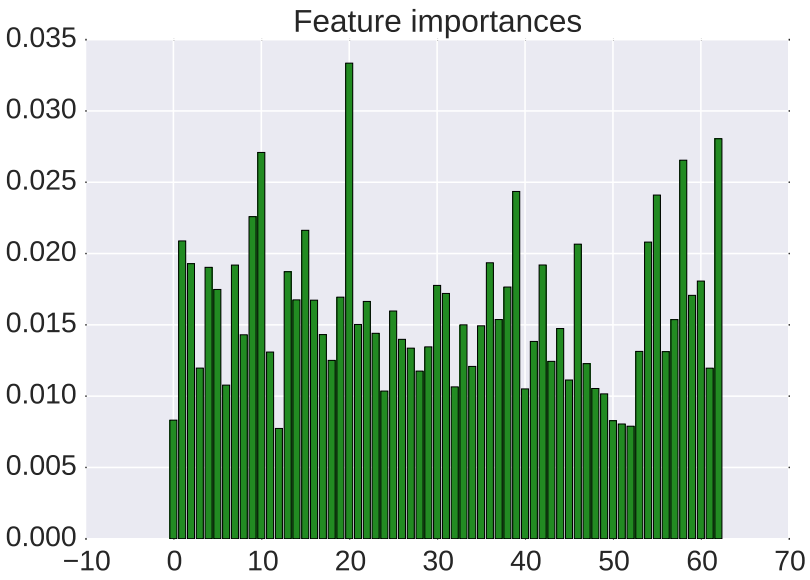

Fig. 27: Feature importance given by the Random Forest Regressor, Inconel 718, SGA, HPC.

In Table. 28 the most important eleven features are shown.

Feature number	Feature name	Related force	Feature importance
20	number of minimum peaks	F_x	0.033352
62	number of minimum peaks	F_z	0.028051
10	minimum of minimum peaks	F_x	0.027090
58	median of minimum peaks	F_z	0.026547
39	kurtosis of minimum peaks	F_y	0.024355
55	variance of maximum peaks	F_z	0.020804
9	minimum of maximum peaks	F_x	0.022586
15	median of maximum peaks	F_x	0.021630
1	minimum	F_x	0.020886
54	maximum of minimum peaks	F_z	0.020804
46	median	F_y	0.020659

Table 28: The most important features selected by Random Forest Regressor, Inconel 718, LGA, HPC.

In Table 28, the majority of the features correspond to statistical parameters of the peaks distribution and the cardinality of the peaks seem to play a relevant role in the regression. Seven of the eleven features are parameters related to minimum peaks. Kurtosis computed for the minimum peaks of F_y and minimum of maximum peaks of F_x are the features repeated in both reduced feature subspaces described in Table 26 and Table 28.

Fig. 28. shows the predicted cumulative flank wear and real flank wear for the second test of Inconel LGA HPC lubrication.

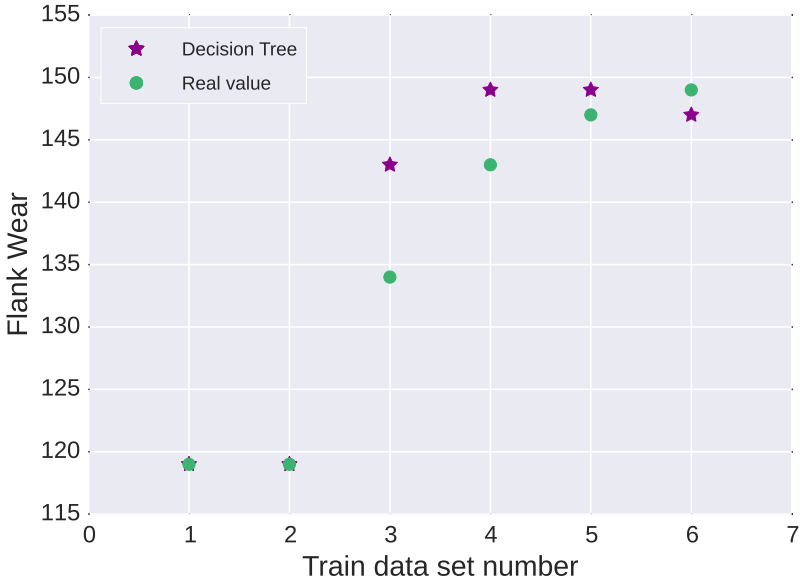

Fig. 28: Real and predicted values of flank wear using Decision Tree (with 11 features) and real values of cumulative flank wear for Inconel 718, LGA, HPC.

The curve generated by the real flank wear points is an increasing curve and the predictions are able to learn that tendency except for the last pass. In some of the cases the predicted and real values are really close to each other. The MSE obtained for Decision Tree Regressor was 20.83.

In this section we have applied predictive regression methods to data obtained from LGA state normal and HPC lubrication. If we compare the values achieved for the maximum flank wear in both of the cases, in using normal lubrication the values are considerably higher that in HPC. In the case of HPC, the maximum values are reached in the sixth pass and the pattern is similar for both of the tests; though for normal lubrication the flank wear for the sixth pass is higher in the second test. One of the reached conclusion in Section 4.1 was that the tests were more similar between them in HPC lubrication than in normal lubrication. The better results obtained for HPC lubrication can be attributed to the mentioned fact. There are two features that appeared in both reduced subspaces: minimum of maximum peaks of F_x and kurtosis of minimum peaks of F_y.

6.4 Small Grain Aged

In this section the same methodology that has been used in Section 6.2 will be applied to Small Grain Aged state for normal and HPC lubrication. In the case of state SGA three tests for each type of lubrication are available. For normal

lubrication and test number one, data about wear is missing. For that reason, for the mentioned state and normal lubrication we will use two tests. From here on, only the figure that corresponds to the model for which the best MSE value has been achieved will be shown.

6.4.1 Normal Lubrication

We will start with SGA state normal lubrication, and for that analysis the tests used are: Inconel 718, SGA, NORMAL, T2 and T3. Table 29 shows the MSE of the methods.

Regressors	MSE
Random Forests	2283.58
Linear Regression	56747.25
Ada Boost	3207.49
k Neighbours	1950.55
Bagging	5238.83
Decision Tree	3091.08
Gradient Boosting	1335.22

Table 29: Mean squared error in prediction of the flank wear for each of the regressors, Inconel 718, SGA, NORMAL.

The analysis of Table 29 shows that the MSE values obtained are higher than the ones obtained for LGA normal lubrication. This phenomenon could be interpreted as LGA tests are more similar between them than SGA tests. The lower MSE achieved correspond to the Gradient Boosting Regressor. As it has occurred in LGA state, linear regression was the worst method. This finding supports the relevance that have the interactions between features in predicting the flank wear.

As we have done before we are going to compute the feature importance using the Random Forest Regressor for the first test, and train and test the regressors with the reduced feature subspace for the second. Table 30 shows the fifteen most important features.

Feature number	Feature name	Related force	Feature importance
62	number of minimum peaks	F_z	0.039885
19	number of minimum peaks	F_x	0.030493
41	number of minimum peaks	F_y	0.027503
21	mean	F_x	0.026255
4	median	F_x	0.025868
12	maximum of minimum peaks	F_x	0.023882
20	number of minimum peaks	F_x	0.023688
26	slope	F_y	0.023180
55	variance of minimum peaks	F_z	0.022635
18	kurtosis of minimum peaks	F_x	0.022365
24	variance	F_y	0.022349
31	minimum of minimum peaks	F_y	0.021864
9	minimum of maximum peaks	F_x	0.020581
10	minimum of minimum peaks	F_x	0.020427
13	variance of maximum peaks	F_x	0.020079

Table 30: The most important features selected by Random Forest Regressor, Inconel 718, SGA, NORMAL.

In Table 30, the first three most important features correspond to the cardinality of the minimum peaks. As it has occurred in section 6.3, there are more features related with the minimum peaks than with the maximum peaks. In addition, there are more features describing the distribution of the peaks than describing the general performance of the forces.

As the results do not improve with less features, in Fig. 29 the real and predicted values are shown for Gradient Boosting Regressor using the original feature space.

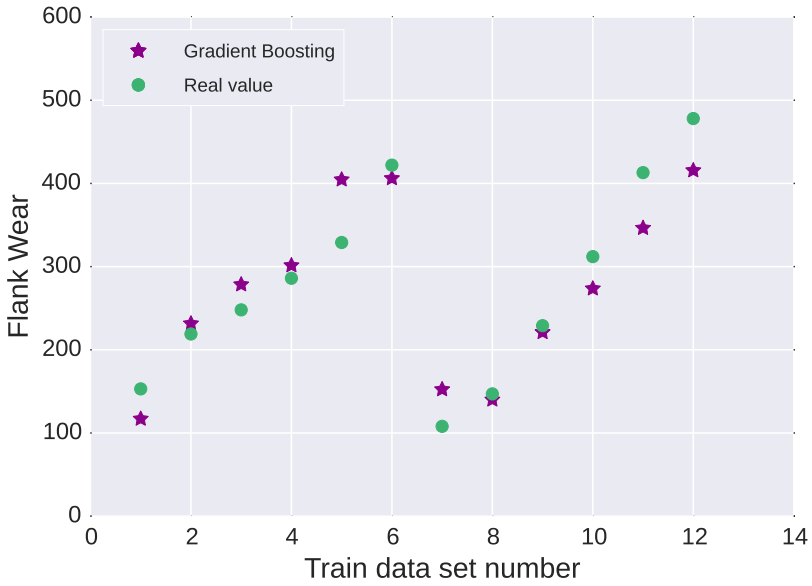

Fig. 29: Real and predicted values of flank wear using Gradient Boosting Regressor, Inconel 718, SGA, NORMAL.

In Fig. 29, we observe that for the first test the predicted values take higher values in general except for the first and last passes. However, for the second test, the predictions are lower than the real values except for the first pass. In this case the tool's critical flank wear ($300\mu m$) is reached after the fourth pass.

6.4.2 High Pression Lubrication

In the case of HPC lubrication, there are available 3 tests so that we have 18 samples. The input matrix dimension is 18×63 as the rows correspond to test cases or samples and the columns to the features. As we can see in Fig. 30, the signals are considerably softer and the peaks seem to be less sharp.

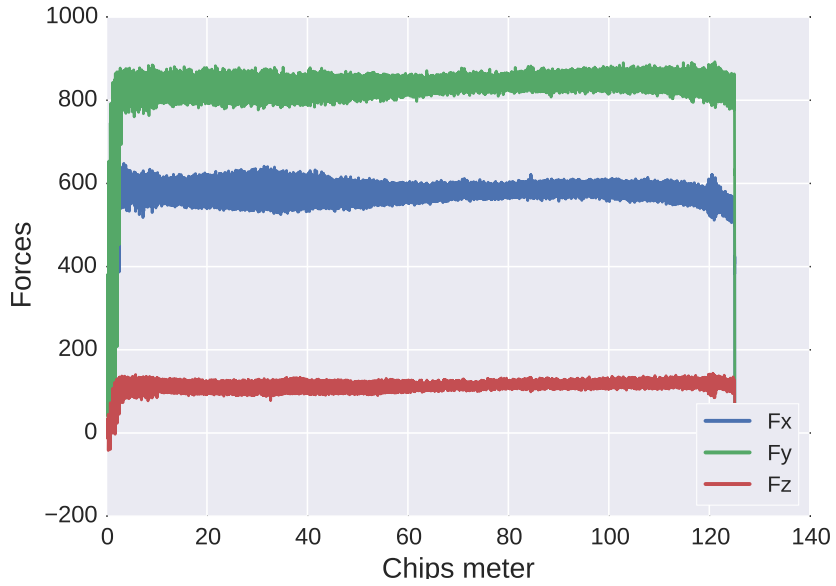

Fig. 30: Forces in Inconel 718, SGA, HPC, T2, pass 1.

Table 31 shows the MSE values obtained from the applied regression methods.

Regressors	MSE
Random Forests	141.56
Linear Regression	278.95
Ada Boost	141.01
k Neighbours	146.60
Bagging	275.05
Decision Tree	307.50
Gradient Boosting	97.81

Table 31: Mean squared error in prediction of the flank wear for each of the regressors, state SGA and HPC lubrication

The analysis of Table 31 shows that the MSE obtained from the methods is lower than the one obtained for data corresponding to normal lubrication. Fig. 31. shows real and predicted values for Gradient Boosting Regressor with the original feature space.

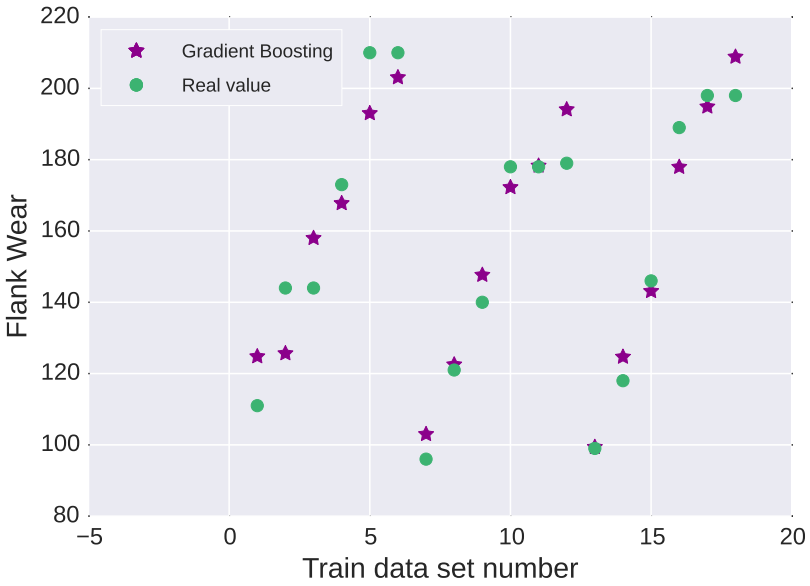

Fig. 31: Real and predicted values of flank wear using Gradient Boosting Regressor, Inconel 718, SGA, HPC.

We observe in Fig. 31 that the prediction for the sixth pass is higher than the real value for test 2 and test 3 and the predictor is able to learn the increasing tendency of the flank wear for one pass to the next. There are some cases, such as pass 2 and 5 from test 2, and pass 1,3 and 5 from test 3, in which the prediction reaches the exact value.

As we have done before, Random Forest Regressor has been applied to the first two tests to compute feature importance. Table 32 shows the most important feature list using as a threshold $\lambda = 0.025$.

Feature number	Feature name	Related Force	Feature importance
33	maximum of minimum peaks of	F_y	0.041207
40	number of maximum peaks	F_y	0.037089
27	kurtosis	F_y	0.035564
34	variance of maximum peaks of	F_y	0.030151
41	number of minimum peaks	F_y	0.029909
61	number of maximum peaks	F_z	0.027606
57	median of maximum peaks	F_z	0.026286
19	number of maximum peaks	F_x	0.026138
3	variance	F_x	0.025207

Table 32: The most important features selected by Random Forest Regressor, Inconel 718, SGA, HPC.

In Table 32, we can see that the majority of the features correspond to the force F_y and there are two features related with the general performance of the forces. In this case there are more features related with maximum peaks than with minimum peaks. As there is no better performance in terms of MSE using the reduced feature subspace we will remain with the results obtained at first.

In this section, the predictions for SGA state normal and HPC lubrication have been obtained. As it has occurred with LGA state when HPC lubrication was used, the prediction of the flank wear was better in terms of MSE. In the case of SGA state, both reduced subspaces (normal and HPC) have two features in common: number of minimum peaks of F_y and number of maximum peaks of F_x.

6.5 Large Grain Solutioned

In this section we apply regression methods presented in section 6.1 for large grain solutioned state. There is no data available for HPC lubrication so that normal lubrication will be investigated. The tests used are Inconel 718, LGS, NORMAL T1 and T2. The MSE values obtained are shown in Table 33.

Regressors	MSE
Random Forests	22115.16
Linear Regression	3510771.67
Ada Boost	29349.20
k Neighbours	22299.32
Bagging	30086.35
Decision Tree	2501.59
Gradient Boosting	12899.64

Table 33: Mean squared error in prediction of the flank wear for each of the regressors, Inconel 718, LGS.

The MSE values are very large for all of the cases. The lowest achieved is for the Decision Tree Regressor. As previously done, feature importance from the Random Forest Regressor will be computed. In Table 34 the most important features are shown using as a threshold $\lambda = 0.02$.

Feature number	Feature name	Related force	Feature importance
34	variance of maximum peaks	F_y	0.035150
55	variance of maximum peaks	F_z	0.027829
9	minimum of maximum peaks	F_x	0.027411
41	number of minimum peaks	F_y	0.025569
1	minimum	F_x	0.024324
20	number of minimum peaks	F_x	0.023162
39	kurtosis of minimum peaks	F_y	0.022669
13	variance of maximum peaks	F_x	0.021719
27	kurtosis	F_y	0.020825
12	maximum of minimum	F_x	0.020784
57	median of maximum peaks	F_z	0.020690
5	slope	F_x	0.020286

Table 34: The most important features selected by Random Forest Regressor, Inconel 718, LGS.

As it has occurred with the states studied before, the statistical parameters derived from the peaks distribution are more important than the statistical parameters that describe the general performance of the forces. The first two most important features are related with the variance of maximum peaks and the parameters related with maximum or minimum peaks distribution are balanced. The majority of the features correspond to the force F_x.

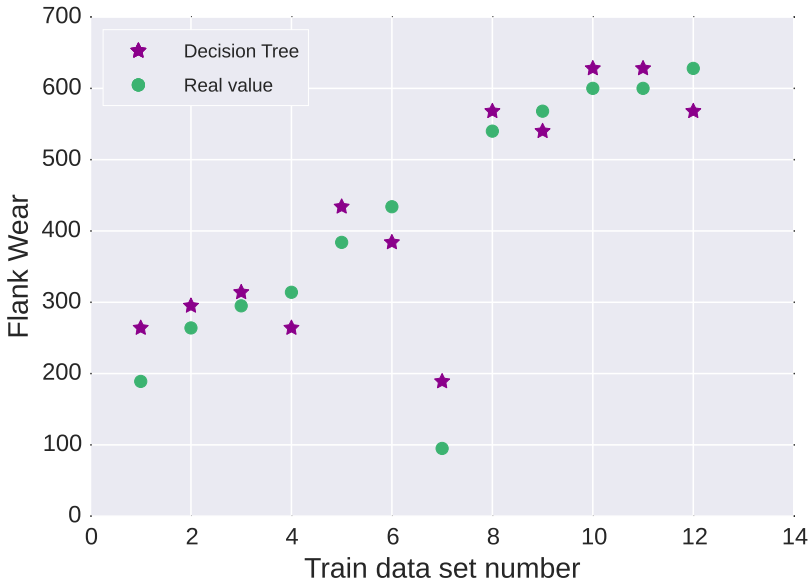

Fig. 32: Real and predicted values of flank wear using Decision Tree Regressor, Inconel 718, LGS.

As there was not an improvement in terms of MSE using the reduced feature subspace, in Fig. 32 the prediction using the original feature space is shown. The real values from the second test do not seem to be reliable because of the presence of a huge jump from pass 1 to pass 2. The low quality of the predictions may be associated with this mentioned phenomenon.

6.6 Small Grain Solutioned

To finish with this section, the prediction of the flank wear for small grain solutioned state will be carried out. As it occurs with LGS state there are not available experiments with HPC lubrication. The tests used to learn the predictive models are Inconel 718, SGS, NORMAL T4 and T5.

Regressors	MSE
Random Forests	8994.88
Linear Regression	4973.68
Ada Boost	7859.47
k Neighbours	8379.38
Bagging	21840.87
Decision Tree	12737.32
Gradient Boosting	10955.71

Table 35: Mean squared error in prediction of the flank wear for each of the regressors, Inconel 718, SGS.

In Table 35, the MSE obtained from the predictions made by the regressors is shown. In this case the obtained values are the highest ones of the all states and lubrications considered. The lowest value corresponds to the Linear Regression. Fig. 33 shows the predicted and real values for the mentioned regression method.

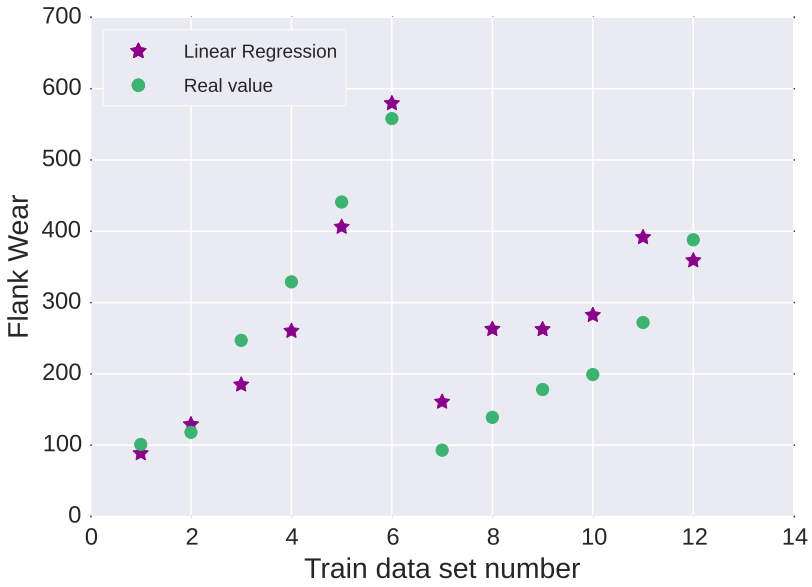

Fig. 33: Real and predicted values of flank wear using linear regression, Inconel 718, SGS.

An analysis of the Fig. 33 shows that for the first test, the predictive values are almost in every pass lower than the real one, except for the last case. However, for the second test, the predictive values are higher except for the last pass.

The list of the most important features, after computing Random Forest Regressor, is shown in Table. 36. However, there is no improvement in the prediction with the reduced subspace.

Feature number	Feature name	Related Force	Feature importance
5	slope	F_x	0.035175
12	maximum of minimum peaks	F_x	0.032480
11	maximum of maximum peaks	F_x	0.024493
4	median	F_x	0.023359
55	variance of maximum peaks	F_z	0.023359
56	variance of minimum peaks	F_z	0.023247
28	mean of maximum peaks	F_y	0.023059
22	minimum	F_y	0.022424
60	kurtosis of minimum peaks	F_z	0.022275
16	median of minimum peaks	F_x	0.021818
43	minimum	F_z	0.021646
25	median	F_y	0.021478
0	mean	F_x	0.021387
9	minimum of maximum peaks	F_x	0.021250
21	mean	F_y	0.020656
62	number of minimum peaks	F_z	0.020242
33	maximum of minimum peaks	F_y	0.020044

Table 36: The most important features selected by Random Forest Regressor, state SGS.

In this state there are more features related with the general performance of the forces than in the states studied before. It is relevant that the first four most important features correspond to the force F_x.

We conclude that the predicted models are not very accurate in the states of solutioned microhardness. In the case of LGS the reason may be that the measurements for the second test are not correct due to human errors. There are four features that are repeated for LGS and SGS states: slop of F_x, maximum of minimum peaks of F_x, minimum of maximum peaks of F_x and variance of maximum peaks of F_z. The feature number nine (minimum of maximum of peaks of F_x) has been repeated for the states LGA, LGS and SGS.

Prediction for the maximum flank wear using features from forces was carried out in this section. For that purpose, seven regression methods were applied and validated. The best results in terms of MSE have been obtained for the

high pressure lubrication (states LGA and SGA). The feature importance computed by Random Forest Regressor has provided us information about the most influential input parameters in predicting flank wear.

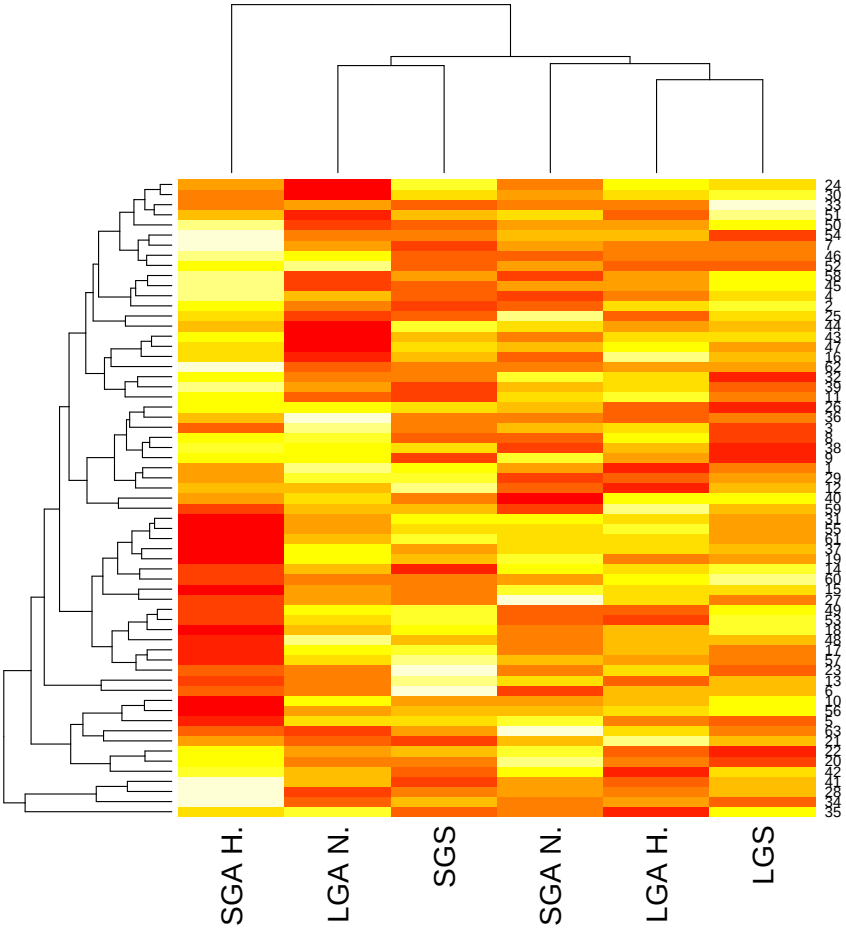

Fig. 34: Heatmap with the feature importance given by the Random Forest Regressor for each of the states considered.

In Fig. 34, a heatmap with the feature importance given by the Random Forest Regressor is showed. The tree diagrams that are at the top and at the left of the heatmap are called dendrograms, and illustrate the arrangement of the clusters produced by hierarchical clustering. If we observe the dendrogram of the states, there are three clusters where, SGA normal, LGA HPC and LGS belong to one cluster, LGA normal and SGS to another cluster and SGA HPC to the third cluster.

It is more difficult to decide how many clusters are comprised in the dendrogram of the left. It can be observed that features 28, 34 and 35 are apart from the rest. The mentioned features are the following ones: mean of maximum peaks of F_y, variance of maximum peaks of F_y and variance of minimum peaks of F_y.

6.7 An improved wear prediction approach

In order to improve the wear prediction performance we propose the following method. As mentioned before the flank wear exhibits an increasing tendency and the values predicted by the different regression approaches are not always able to follow that tendency. The proposed approach uses this knowledge about the specific context in which regression is applied (i.e. the regressed function is assumed to be monotonically non-decreasing). We take into account two different scenarios; in the first one the real flank wear is measured after each pass, i.e. wear is predicted for time t, the turning process is applied, and then wear is measured and can be contrasted with the prediction. In the second scenario, we know the real flank wear measurements only at the end of the process.

In the first scenario we propose computing the predicted flank wear in pass t in the following way:

$$\hat{p}_t = max(p_t^*, p_{t-1}) \tag{7}$$

Where p_t^* is the predicted flank wear obtained from the regression method in pass t and p_{t-1} is the observed flank wear. In this way we ensure that the predicted flank wear does not decrease.

In the second scenario, as the measurements are not done at the moment, we compute the predicted flank wear in pass t in the following way:

$$\hat{p}_t = max(p_t^*, p_{t-1}^*) \tag{8}$$

Where p_t^* is the predicted flank wear obtained from the regression method in pass t and p_{t-1}^* is the predicted flank wear obtained from the regression method in pass $t-1$.

We are going to apply the explained approach to Inconel 718, LGA, HPC test 1 and test 2 datasets. The reason for choosing these tests is that although the difference between predicted and real values of flank wear are quite similar, there are points in which the flank wear value predicted for time t is lower than

the one predicted for time $t-1$. We will use test 1 to learn the predicted model and test 2 to evaluate.

In the case of LGA state and HPC lubrication, the Gradient Boosting Regressor was the regression method that perform best. We are going to use test 1 to learn the model and test 2 to validate. The achieved MSE value without taking into account the proposed scenarios is, 425.04. However, the MSE in the first scenario is 82.48 and in the second scenario 408.08. Therefore, by considering this information about the specific characteristics of the measurements being approximated, we can improve the quality of the prediction.

Fig. 35 shows the predicted and real values from the first scenario as it has the lowest MSE value. Notice, how non-monotonicity is enforced, the method use the real values of previous measurements to correct the predictions at the current pass.

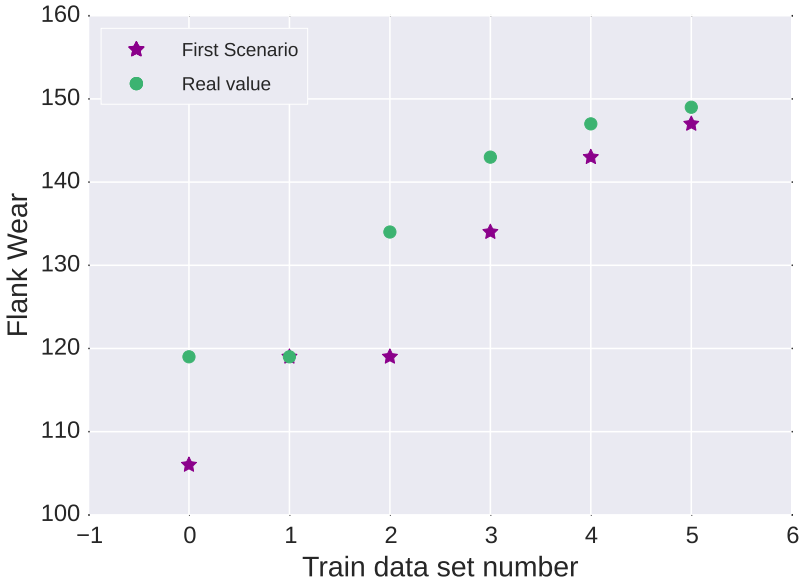

Fig. 35: The improved wear prediction for the first scenario using Gradient Boosting Regressor, Inconel 718, LGA, HPC.

7 Conclusions

In this thesis we have addressed the problem of tool wear in the turning process of Inconel 718. For that purpose a statistical analysis of the flank wear has been accomplished followed by the investigation of some machine learning algorithms

in the task of predicting the flank wear. The statistical analysis of the flank wear has included a hypothesis testing technique, more specifically the Wilcoxon signed-rank test, to study the influence of the material characteristics on the tool wear. Before applying the regression methods to predict the flank wear, a feature selection procedure of the cutting forces has been carried out. Additionally, a comparison of the different variants of the algorithms implemented has been made and the prediction of the wear has also served to study the influence that the material characteristics have on the flank wear. In this section the main contributions of this work will be presented.

Firstly, principal component analysis was applied to Inconel 718 material for all states and lubrications considered as a part of an exploratory data analysis. This analysis was carried out for the data collected at beginning and the end of the process to observe the evolution of the forces. The explained percentage of variance achieved was very high in all the cases and it was found that in the case of LGA and SGS states the explained variance percentage decreases from pass 1 to pass 6. In the case of SGA and LGS state the inverse pattern was detected. To deal with lower dimensionality of samples PAA was computed. The findings of this analysis can be classified into two types: 1) In a particular test and pass, PCA can be used to filter the data (remove the initial peak) 2) The differences that exist among the states of the material and lubrication have revealed the necessity to generate particular predictive models for each of the cases. The analysis also revealed that in SGA state and HPC lubrication, the projected force had similar shape in the three available tests.

Cutting tool life and wear is an important consideration in metal cutting processes. There are some factors that have influence on tool wear such as: Cutting tool geometry, cutting conditions, cutting tool material and workpiece material. The material utilized achieves four states that are differentiated in grain size and hardness. To analyze the effect that those factors have in the flank wear statistical hypothesis testing was applied. The reached conclusion was that grain size has bigger influence on wear when the hardness was aged than when was solutioned. In the case of microhardness, it had impact on wear for small grains whereas it had not for large grains. In respect of lubrication, there was a significant difference in using normal or HPC lubrication. The fact that there are significant differences between normal and HPC lubrication has justified the remarkably different results obtained in the predictions.

Development of a predictive model for wear prediction including the effect of the forces is an extremely difficult task due to the non-linear behavior of the wear mechanism. There are several factors that have an impact on wear and a proper analysis of the relationship between the forces and flank wear was required. For that purpose Pearson's correlation coefficient was used. It was found that features obtained from forces F_x and F_y present higher correlation with flank wear than those obtained from F_z in almost every case. There was a high correlation between the variance of the forces and flank wear and between slope of the forces and flank wear. As long as the force distances from the mean value the flank

wear increased. The number of maximum and minimum peaks presented also a strong correlation with flank wear and a larger number of peaks implied lower flank wear. Also the variance and kurtosis of the peaks were correlated with flank wear. Our analysis could be useful at the time of selecting which are the most informative features for estimating tool wear in other superalloys.

One of the main objectives of this thesis has been to generate a predictive model for tool wear. The analysis carried out before solving the prediction problem has revealed the complexity of the turning process and the differences that exist among the states and lubrications used. Some regression methods have been applied in order to predict the maximum flank wear employing leave-one-out cross-validation technique to define train and test sets. In some of the cases, the prediction performance has been improved using a machine learning feature selection step based on feature importance of the Random Forest Regressor.

Remarkably better results were obtained for HPC lubrication than for normal lubrication in both states (LGA and SGA) that consider HPC lubrication. For the aged hardness, the regression methods for large grain state perform better than small grain state. In the case of LGA state, an improvement was achieved with the features learnt using the Random Forest Regressor. This finding reveals, that in this case, the selected features from the forces serve to characterize the machining process. However, the predictive models are not accurate in the case of solutioned hardness. In the case of LGS state, this issue can be attributed to the human errors made in the measurement of the flank wear. The majority of the important features correspond to F_x, followed by F_y and finally F_z. In total, there are more statistical parameters in important features that correspond to the minimum peaks than to the maximum peaks. The comparison of the algorithms implemented on data reveals that the Gradient Boosting Regressor predominates in almost every case over the rest of the machine learning algorithms.

This thesis has revealed the necessity to expand the research with HPC lubrication as the best results in terms of MSE were achieved for this scenario. This would be a necessary step to the creation of more efficient machining processes. The forces F_x and F_y seem to be more relevant in characterizing the machining process than F_z but more studies in this direction would be required. The presented research can be improved extending the quantity of input variables such as the temperature.

References

1. T. Anderson. *The Statistical Analysis of Time Series.* Wiley, 1994.
2. Y. Arisoy and T. Ozel. Machine learning based predictive modeling of machining induced microhardness and grain size in Ti–6Al–4V Alloy. *Materials and Manufacturing Processes*, 30:425–433, 2015.
3. P. Arrazola, T. Özel, D. Umbrello, M. Davies, and I. Jawahir. Recent advances in modelling of metal machining processes. *Manufacturing Technology*, 62:695–718, 2013.
4. A. Attanasio, E. Ceretti, and C. Giardini. Analytical models for tool wear prediction during AISI 1045 turning operations. *Procedia CIRP*, 8:218–223, 2013.
5. G. Boothroyd and W. Knight. *Fundamentals of machining and machine tools.* Marcel Dekker, 1988.
6. E. Bradley. *Superalloys: a technical guide.* ASM International, Metals Park, OH, 1988.
7. L. Breiman. Random forests. *Machine Learning*, 45:5–32, 2001.
8. L. Breiman, J. Friedman, R. Olshen, and C. Stone. *Classification and regression trees.* Chapman and Hall/CRC, 1984.
9. R. Buckson and O. Ojo. Cyclic deformation characteristics and fatigue crack growth behavior of a newly developed aerospace superalloy Haynes 282. *Materials Science and Engineering*, 55:63–70, 2012.
10. M. Chandrasekaram and C. M. Krishna. Application of soft computation techniques in machining performance prediction and optimization: a literature review. *The International Journal of Advanced Manufacturing Technology*, 46:445–464, 2010.
11. S. Choudhury and K. Kishore. Tool wear measurement in turning using force ratio. *International Journal of Machine Tools & Manufacture*, 40:899–909, 2000.
12. G. Chryssolouris and M. Guillot. A comparison of statistical and AI approaches to the selection of process parameters in intelligent machining. *ASME J Eng Ind*, 112:112–131, 1990.
13. O. Colak. Investigation on machining performance of Inconel 718 under high pressure cooling conditions. *Journal of Mechanical Engineering*, 58:683–690, 2012.
14. M. Correa, C. Bielza, and J. Pamies-Teixeira. Comparison of bayesian networks and artificial neural networks for quality detection in a machining process. *Expert Systems with Applications*, 36:7270–7279, 2009.
15. J. Davim. *Machining; fundamentals and recent advantages.* Springer, 2008.
16. A. K. Dubey and V. Yadava. Multi-objective optimization of Nd: YAG laser cutting of nickel-based superalloy sheet using orthogonal array with principal component analysis. *Optics and Lasers in Engineering*, 46:124–132, 2008.
17. D. Dudzinski, A. Devillez, A. Moufki, D. Larrouquere, V. Zerrouki, and J. Vigneau. A review of developments towards dry and high speed machining of Inconel 718 alloy. *Machine tools & manufacture*, 44:439–456, 2004.
18. G. H. Dunteman. *Principal Component Analysis.* Sage, 1989.
19. E. Ezugwu, D. Fadare, J. Bonney, and W. S. R.B. Da Silva. Modelling the correlation between cutting and process parameters in high-speed machining of Inconel 718 alloy using an artificial neural network. *Machine Tools & Manufacture*, 45:1375–1385, 2005.
20. C.-X. Feng and X.-F. Wang. Surface roughness predictive modelling: neural networks versus regression. *IEE Trans*, 35:11–27, 2003.

21. J. Friedman. Stochastic gradient boosting. *Computational Statistics & Data Analysis*, 38:367–378, 2002.
22. S. García, A. Fernández, J. Luengo, and F. Herrera. Advanced nonparametric tests for multiple comparisons in the design of experiments in computational intelligence and data mining: Experimental analysis of power. *Information Sciences*, 180:2044–2064, 2010.
23. C. Guo, H. Lin, and D. Pan. An improved piecewise aggregate approximation based on statistical features for time series mining. In *Knowledge Science, Engineering and Management*, pages 234–244. Springer Berlin Heidelberg, 2010.
24. M. A. Hall. *Correlation-based Feature Selection for Machine Learning*. PhD thesis, The University of Wakaito, April 1999.
25. C. Hu, G. Jain, P. Zhang, C. Schmidt, P. Gomadam, and T. Gorka. Data-driven method based on particle swarm optimization and k-nearest neighbor regression for estimating capacity of lithium-ion battery. *Applied Energy*, 129:49–55, 2014.
26. B. Kaya, C.Oysu, and HM.Ertunc. Force torque based on-line tool wear estimation system for CNC milling of Inconel 718 using neural networks. *Advances in Engineering Software*, 42:76–81, 2011.
27. B. Kilundu, P. Dehombreaux, and X. Chiementin. Tool wear monitoring by machine learning techniques and singular spectrum analysis. *Mechanical Systems and Signal Processing*, 25:400–415, 2011.
28. R. Kohavi. A study of cross-validation and bootstrap for accuracy estimation and model selection. 2001.
29. K. M. Lavanya, R.K.Suresh, A. K. Priya, and V. Reddy. Optimization of process parameters in turning operation of AISI-1016 Alloy steels with CBN using taguchi method and anova. *Journal of Mechanical and Civil Engineering*, 7, 2013.
30. M. Lotfi, M. Jahanbakhsh, and A. Farid. Wear estimation of ceramic and coated carbide tools in turning of Inconel 625: 3D FE analysis. *Tribology International*, 99:107–116, 2016.
31. C. Lu. Study on prediction of surface quality in machining process. *Journal of materials processing technology*, 205:439–450, 2008.
32. P. Mahadeo and U.Shanker. *Modeling of Metal Forming and Machining Processes; by Finite Element and Soft Computing Methods*. Springer, 2008.
33. A. Mitrofanov, N. Ahmed, V. Babitsky, and V. Silberschmidt. Effect of lubrication and cutting parameters on ultrasonically assisted turning of Inconel 718. *Journal of Materials Processing Technology*, 162-163:649–654, 2005.
34. H. Motoda and H. Liu. *Feature extraction, construction and selection*. Kluwer academic publishers, 1998.
35. S. Olovsjö and L. Nyborg. Influence of microstructure on wear behavior of uncoated WC tools in turning of Alloy 718 and Waspaloy. *Wear*, pages 12–21, 2012.
36. S. Olovsjö, A. Wretland, and G. Sjöberg. The effect of grain size and hardness of wrought Alloy 718 on the wear of cemented carbide tools. *Wear*, 268:1045–1052, 2010.
37. L. Osoba and O. Ojo. Influence of laser welding heat input on haz cracking in newly developed haynes 282 superalloy. *Materials Science and Technology*, 28(4):431–436, 2012.
38. R. Pawade, S. S. Joshi, and P. Brahmankar. Effect of machining parameters and cutting edge geometry on surface integrity of high-speed turned Inconel 718. *Machine Tools & Manufacture*, 48:15–28, 2008.
39. F. Pedregosa, G. Varoquaux, A. Gramfort, V. Michel, B. Thirion, O. Grisel, M. Blondel, P. Prettenhofer, R. Weiss, V. Dubourg, J. Vanderplas, A. Passos,

D. Cournapeau, M. Brucher, M. Perrot, and E. Duchesnay. Scikit-learn: Machine learning in Python. *Journal of Machine Learning Research*, 12:2825–2830, 2011.
40. R. Pino-Mejías, M. Jiménez-Gamero, M. C. de-la Vega, and A. Pascual-Acosta. Reduced bootstrap aggregating of learning algorithms. *Pattern Recognition Letters*, 29:265–271, 2008.
41. K. Prasad. Influence of cutting parameters on turning process using Anova analysis. *Research journal of engineering sciences*, 9:1–6, 2013.
42. Y. Qian, J. Tian, L. Liu, Y. Zhang, and Y. Chen. A tool wear predictive model based on SVM. In *Chinese Control and Decision Conference*, page 1213–1217, 2010.
43. S. Rangwala and D. Dornfeld. Learning and optimization of machining operations using computing abilities of neural networks. *IEEE Trans Syst Man Cybern*, 19:299–314, 1989.
44. R. Reed. *The Superalloys: Fundamentals and Applications*. Cambridge University Press, 2008.
45. R. Schapire. *The boosting approach to machine learning: an overview*. Springer, 2003.
46. F. Scholkmann, J. Boss, and M. Wolf. An efficient algorithm for automatic peak detection in noisy periodic and quasi-periodic signals. *Algorithms*, 5:588–603, 2022.
47. G. A. Seber and A. J. Lee. *Linear Regression Analysis*. Wiley, 2003.
48. T. Segreto, A. Simeone, and R. Teti. Sensor fusion for tool state classification in nickel superalloy high performance cutting. In 5^{th} *CIRP Conference on High Performance Cutting 2012*, pages 593–598, 2012.
49. T. Segreto, A. Simeone, and R. Teti. Principal component analysis for feature extraction and NN pattern recognition in sensor monitoring of chip form during turning. *Journal of Manufacturing Science and Technology*, 7:202–209, 2014.
50. D. Shi and N. Gindy. Tool wear predictive model based on least squares support vector machines. *Mechanical systems and signal processing*, 21:1799–1814, 2007.
51. S. Sikdar and M. Chen. Relationship between tool flank wear area and component forces in single point turning. *Journal of Materials Processing Technology*, 128:210–215, 2002.
52. R. Slavkovic, S. Arsovski, and A. Jovicic. A study of wear rate estimation of casting parts by support vector machine. In 16^{th} *International Research/Expert Conference*, pages 619–622, 2012.
53. R. Slavkovic, Z. Jugovic, S. Dragicevic, A. Jovicic, and V. Slavkovic. An application of learning machine methods in prediction of wear rate of wear resistant casting parts. *Computers & Industrial Engineering*, 64:850–857, 2013.
54. A. Suárez, F. Veiga, L. L. de Lacalle, R. Polvorosa, and A. Wretland. An investigation of cutting forces and tool wear in turning Haynes 282. Unpublished manuscript, 2016.
55. A. Suárez, F. Veiga, L. L. de Lacalle, R. Polvorosa, and A. Wretland. Machining performance analysis of nickel-based alloys, Alloy 718 and Waspaloy, at different level of coolant pressure. Unpublished manuscript, 2016.
56. A. Suárez, F. Veiga, L. L. de Lacalle, R. Polvorosa, and A. Wretland. Variation of wear pattern in high-pressure cooling face-turning of Alloy 718. Unpublished manuscript, 2016.
57. J. Suykens and J. Vandewalle. Least squares support vector machine classifiers. *Neural Processing Letters*, 9:293–300, 1999.
58. V. Vapnik. *The Nature of Statistical Learning Theory*. Springer, New York, 1999.

59. N. Vaxevanidis, J. Kechagias, N. Fountas, and D. Manolakos. Three component cutting force system modelling and optimization in turning of AISI D6 tool steel using design of experiments and neural networks. In *Proceedings of the World Congress on Engineering*, pages 629–633, 2013.
60. V. Vijayaraghavan, A. Garg, L. Gao, R.Vijayaraghavan, and G. Lu. A finite element based data analytics approach for modeling turning process of Inconel 718 alloys. *Journal of cleaner production*, 30:1–9, 2016.
61. J. Wang, P. Wang, and R. Gao. Enhanced particle filter for tool wear prediction. *Journal of manufacturing systems*, 36:35–45, 2015.
62. M. Xu, P. Watanachaturaporn, P. Varshney, and M. Arora. Decision tree regression for soft classification of remote sensing data. *Remote Sensing of Environment*, 97:322–336, 2005.
63. R. Yadav, K. Abhishek, and S. Mahapatra. A simulation approach for estimating flank wear and material removal rate in turning of Inconel 718. *Simulation modelling practice and theory*, 52:1–14, 2015.
64. Y. Yen, J. S*öhner*, B. Lilly, and T. Altan. Estimation of tool wear in orthogonal cutting using the finite element analysis. *Journal of Materials Processing Technology*, 146:82–91, 2004.
65. N. Yusup, A. Zain, and S. Hashim. Evolutionary techniques in optimizing machining parameters: Review and recent applications (2007-2011). *Expert Systems with Applications*, 39:9909–9927, 2012.
66. D. Zhu, X. Zhang, and H. Ding. Tool wear characteristics in machining of nickel-based superalloys. *Machine Tools & Manufacture*, 64:60–77, 2013.
67. O. Zienkiewicz. *The finite element method*. London: McGraw-Hill, 1977.